THE MINERALOGICAL MAGAZINE

AND

JOURNAL OF

THE MINERALOGICAL SOCIETY

No. 198 September, 1947 Vol. XXVIII

Nigerite, a new tin mineral.

By F. A. Bannister, M.A., Sc.D., F.Inst.P., M. H. Hey, M.A., D.Sc.
Department of Mineralogy, British Museum,

and H. P. Stadler, B.Sc.,
Department of Physical Chemistry, University of Leeds.

[Read January 23, 1947.]

THE discovery of nigerite, a new tin-bearing mineral, by R. Jacobson and J. S. Webb[1] claims more than the passing interest of an addition to the few known species containing appreciable tin. Nigerite is the first mineral to be discovered in which both tin and aluminium are essential constituents. Its chief interest to mineralogists lies in its close relationship to minerals like spinel and corundum based on a close-packed or nearly close-packed assemblage of oxygen ions.

Samples of nigerite submitted to us for investigation consist of brittle, lustrous, brown, weakly magnetic, hexagonal plates up to 5×2 mm. in size but mostly much smaller. These samples also contained grains of cassiterite, columbite, gahnite, sillimanite, quartz, andalusite, and chrysoberyl, which were easily separated by hand-picking. Many nigerite crystals were encountered intergrown with or enclosing cassiterite, columbite, quartz, and sillimanite and these also were set aside as unsuitable for chemical study. A preliminary spectrographic examination, kindly undertaken for us by Mr. B. S. Cooper of the Research Laboratories of the General Electric Company, Wembley, revealed the presence of Sn, Zn, Fe, Al, and Si; and minor amounts of Mn, Li, Mg, and Ti.[2] A separate portion of the mineral was also examined in the

[1] R. Jacobson and J. S. Webb, Min. Mag., 1947, vol. 28, pp. 118–128.

[2] Examination of a separate sample by D. L. Williams in the Museum confirmed these results except for Li and Ti. He also found Pb, Ca, and P. This discrepancy is probably due to non-uniformity of sample.

same laboratories by Mr. L. A. Thomas for piezoelectricity but no positive effect was discovered.

A larger sample also carefully cleaned and hand-picked and containing no visible accessory minerals was then handed to Dr. Hey for complete analysis.

Chemical analysis of nigerite (M. H. Hey).

The material available for analysis (2 grams) contained a small amount of quartz and sillimanite, present as minute inclusions and films on most of the grains, but no other impurities could be observed under the microscope.

Nigerite is insoluble in acids, and is very imperfectly attacked by fusion with sodium carbonate or caustic soda, but readily gives a clear fusion with borax and with sodium pyrosulphate. For the main part of the analysis the mineral was fused with sodium pyrosulphate, and after solution and elimination of SiO_2 the tin was distilled as bromide from the sulphuric acid solution at 200° C.; in the distillate tin was precipitated by NH_3 and weighed as SnO_2. The residue was treated with H_2S and the precipitate examined in the usual manner; it proved to be wholly PbS, which was converted to $PbSO_4$ for weighing. The oxidized filtrate from the sulphides was precipitated by ammonia at *p*H 7, and the precipitate dissolved and reprecipitated twice, ignited and weighed (Al_2O_3, Fe_2O_3, TiO_2, and some ZnO), then fused with sodium pyrosulphate, and iron and titania precipitated with cupferron; after igniting and weighing, the Ti was determined colorimetrically. Ammonium citrate was added to the filtrate from the cupferron precipitate, then ammonia and ammonium sulphide, and the small precipitate of ZnS collected, ignited to ZnO, and weighed, alumina being obtained by difference. In the filtrate from the ammonia precipitate, Zn and Mn were precipitated as sulphides and weighed as oxides, the manganese being determined colorimetrically; calcium was found to be absent, and Mg was determined as 8-hydroxyquinolate and tested for Zn. A second portion was used for determination of loss at 200° C. and on ignition, and for a check tin determination (precipitation of Sn and Pb as sulphides and separation by Am_2S).

The ferrous iron determination by the modified Rowledge method (Min. Mag., 1941, vol. 26, p. 116) encountered unexpected difficulties, the tube swelling up and bursting during fusion; this suggested that the mineral contains a considerable amount of water which is not lost on ignition at about 900° C., and a water determination made in the Gooch

tubulated crucible with anhydrous borax as flux confirmed this. By the kindness of Mr. A. T. Green, Director of the British Refractories Research Association, Dr. G. R. Rigby carried out a Rowledge fusion on nigerite in the Mellor Laboratories, Stoke-on-Trent, using for the purpose an evacuated sealed silica-glass tube, and heating it in an atmosphere of nitrogen, since silica-glass is slightly permeable to gases at 950° C. This result may be somewhat low, since there may have been some oxidation of FeO by the water present, but the effect is not likely to be great.[1] There was no noticeable attack on the silica tube except at the surface of the melt; there, a marked attack was observed, presumably through the co-operation of the flux (B_2O_3+NaF) and water released from the mineral.

The density was determined by the floatation method in Clerici solution; nigerite just floats in saturated Clerici solution, and the density, corrected to vacuum and for 0·48 % quartz, was found to be D_4^{16} 4·51. The hardness is between 8 and 9; the basal plane of a larger crystal can be scratched by corundum, while topaz is abraded.

TABLE I. Chemical analysis of nigerite (I), atomic quotients* (P/M), ionic radii (R), empirical unit-cell contents (II), and atomic ratios to a basis of 24(O,OH) (III). The oxides are given in order of decreasing ionic radius of the metals. Conversion factor* $F=(\frac{1}{2}\sqrt{3}a^2cD)/(1{\cdot}651\times 99{\cdot}35)=10{\cdot}66$.

	I.		P/M	R.	II.	III.		
PbO ...	0·94	Pb ...	0·004	0·84	0·05	0·04		with 0·33 Mg and 0·09 $Fe^{...}$ = 1·24
MnO ...	0·09	Mn ...	0·001	0·80	0·01	0·01		
FeO ...	2·65	$Fe^{..}$ ...	0·037	0·75	0·39	0·39		
ZnO ...	4·51	Zn ...	0·055	0·74	0·59	0·59	0·38	
SnO_2 ...	25·33	Sn ...	0·168	0·71	1·79	1·77	0·21	2·00
TiO_2 ...	0·17	Ti ...	0·002	0·68	0·02	0·02		
MgO ...	1·28	Mg ...	0·032	0·65	0·34	0·33		to $R^{...}$ group
Fe_2O_3 ...	11·90	$Fe^{...}$ ...	0·149	0·60	1·59	1·57	0·09	to $R^{..}$ group
Al_2O_3 ...	50·91	Al ...	0·998	0·50	10·66	10·52	1·48	12·00
H_2O† ...	1·57	OH ...	0·174	—	1·86	1·84		
SiO_2 ...	0·48	O ...	—	—	22·47	22·16		
	99·83‡	∑(O,OH)			24·33	24·00		
		∑(metals).....			15·44	15·24		

* Min. Mag., 1939, vol. 25, p. 403.
† H_2O lost at 200° C., 0·11 %; at 900° C., 0·38 %.
‡ CaO < 0·01 %; P_2O_5, Li_2O, not determined.

[1] This conclusion is supported by the recalculation of the analysis to atomic ratios on a basis of 24(O,OH); if the $Fe^{...}$ is assigned with the Al, the excess over the most probable value of 12·00 is only 0·09, corresponding to 0·72 % Fe_2O_3.

From the analysis and the observed density and unit-cell dimensions, the empirical unit-cell contents and the atomic ratios to a basis of (O,OH) = 24 were calculated. The results (table I) clearly indicate an ideal repeat[1] of $(Zn,Mg,Fe^{\cdot\cdot})(Sn,Zn)_2(Al,Fe^{\cdot\cdot\cdot})_{12}O_{22}(OH)_2$. Calculations based on generously assigned maximum probable errors of the chemical analysis and physical determinations show that the (O,OH) figure must be within the limits 22·8—25·2 and is almost certainly very near 24·0, while the sum of the metal atoms must be between 14·8 and 16·2 and is almost certainly appreciably greater than 15; the structure has, of course, ample interstitial vacancies for this excess of metal atoms over the ideal repeat.

Crystallography of nigerite (F. A. B. and H. P. S.).

All the crystals and crystal fragments of nigerite so far examined possess a brilliantly reflecting basal plane. Trigonal pyramid faces are also developed on some crystals and as the mineral gives a good uniaxial positive figure[2] when examined with the polarizing microscope it was rightly concluded to belong to a trigonal class of the hexagonal system. The reflected images from the pyramid faces are, however, disappointing. Larger crystals yield weak and confused images from all but the basal plane, whilst more perfect small crystals are so thin that the pyramid faces yielding bright reflections to the unassisted eye prove on goniometric examination to be giving diffuse diffracted images. It was, therefore, possible only to index the pyramid forms after X-ray measurement of the axial ratio and no sufficiently accurate independent goniometric value was obtained.

Laue photographs of several hexagonal plates and platy fragments of nigerite are identical and show threefold patterns with planes of symmetry (i.e. three vertical planes parallel to the $c[0001]$ axis). Single crystal rotation photographs of a small hexagonal plate of nigerite set optically with $a[10\bar{1}0]$ and $c[0001]$ axes vertical in turn yield a 5·72 c 13·86 Å. (equivalent to a 5·71, c 13·83 kX). The latter bracketed values have been used by one of us (M. H. H.) with the appropriate factor 1·651 in calculating the unit-cell contents (table I). No systematic halvings of the diffractions observed on oscillation photographs about the $a[10\bar{1}0]$ axis can be found and the possible space-groups,

[1] Zn has been assigned to complete the Sn positions, since it has the nearest ionic radius to Sn of the other metals present.

[2] So far only approximate values of the refractive indices of nigerite have been obtained by the Becke line method, ω 1·80, ϵ 1·81.

taking also Laue symmetry into consideration, are D_{3d}^3—$C\bar{3}$m, D_{3d}^1—$C\bar{3}1m$, D_3^1—$C312$, D_3^2—$C32$, C_{3v}^1—$C3m$, and C_{3v}^2—$C31m$. The axial ratio calculated from the unit-cell dimensions is $a:c = 1:2{\cdot}423$. Both large and small crystals show faces of the trigonal pyramid $(10\bar{1}1)$ the calculated angle for $(0001):(10\bar{1}1)$ being 70° 20′ and observed goniometric values for one of the best-developed but thin crystals of nigerite ranging from 69° 41′ to 72° $3\frac{1}{2}$′. Two other pyramid forms observed on the same crystal are $(10\bar{1}3)$ and a doubtful $(3{\cdot}0{\cdot}\bar{3}{\cdot}16)$. The crystals of nigerite so far encountered show few forms and these, with the sole exception of the basal plane, are poorly developed. This renders the determination of crystal class by goniometric measurement uncertain. There is some probability, from the distribution of the faces observed as well as from the lack of any marked piezoelectricity, that the crystals so far studied do not possess uniterminal axes either in or perpendicular to the basal plane. It may prove, therefore, that the choice of space-group can be restricted by further investigation of crystal form to $C\bar{3}m$ or $C\bar{3}1m$, the only two of the six space-groups given above which are non-polar.

Although no crystal-structure determination of nigerite has so far been attempted, the dimensions and contents of the unit cell, which are the results of the X-ray and chemical study, suggest that the crystal structure will prove to be based upon a nearly close-packed hexagonal arrangement of oxygen and hydroxyl ions. The unit cell of a hexagonal close-pack of oxygen ions each 2·7 Å. in diameter has dimensions a 2·7, c 4·4 Å., the c dimension being twice the height of a tetrahedron of oxygen ions, standing on its base. This unit contains two oxygen ions. If twelve of these units are stacked so that a new cell is constructed containing twenty-four oxygen ions with $a' = 2a$, 5·4 Å. and $c' = 3c$, 13·2 Å., we have an approximation in dimensions to the unit cell of nigerite. The location of the metal ions Sn, Al, Fe, Zn, Mg, &c., in the tetrahedral and octahedral interstices of such an arrangement must be found by X-ray methods and it may prove possible also to discover how the two hydroxyl and twenty-two oxygen ions are distributed over the twenty-four sites of the nearly close-packed hexagonal array of positive ions.

The high refractive index and low birefringence, the hardness, and high specific gravity of nigerite are all properties common to other minerals based upon hexagonal close-packed oxygen assemblages like corundum or chrysoberyl. The value of the refractive index calculated for a close-packed assemblage of oxygen atoms, each 2·7 Å. in diameter, is 1·71

neglecting the contribution of the metal ions.[1] It is reasonable to expect the refractive index of nigerite to be higher than 1·71, for, although it is not quite close-packed, the presence of ions with high refractivity like iron and tin will more than counterbalance the decrease of refractivity due to this expansion.

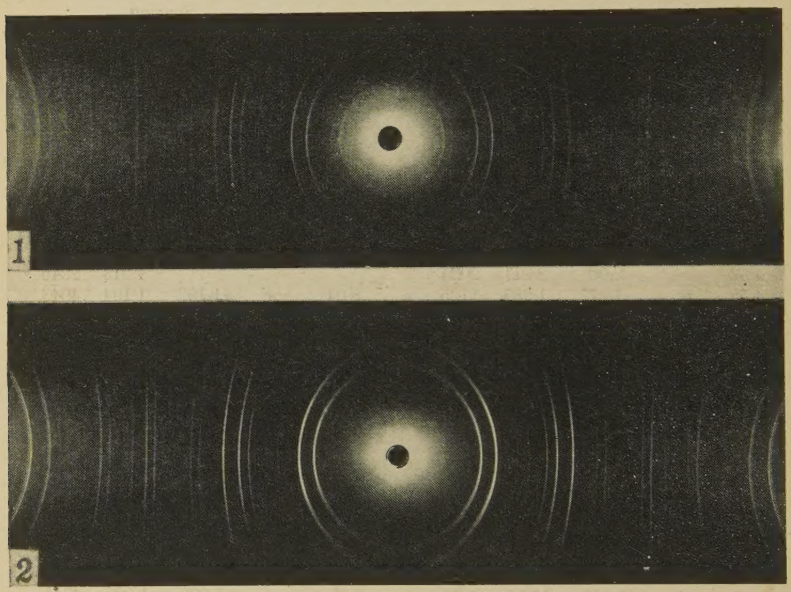

FIG. 1. X-ray powder photographs of nigerite (1) and gahnite (2) from Kabba, Nigeria, taken with filtered copper radiation in a cylindrical camera diameter 6 cm.

The most direct evidence of the hexagonal close-packing of the oxygen and hydroxyl ions in nigerite is afforded, however, by the oriented overgrowth of nigerite on the octahedral planes of gahnite. This spinel has already been described as one of the accessory minerals by Jacobson and Webb, who refer to an octahedron of gahnite coated with nigerite. Each face (111) of this specimen is covered with a single crystal of nigerite. The crystal-structure of the spinels is based upon a cubic close-packing of oxygen ions and it is obvious that a single layer of this cubic arrangement perpendicular to (111) is identical with a single layer of the hexagonal close-packed arrangement perpendicular to (0001). Hence the oxygen ions in the basal plane of nigerite can fit exactly to

[1] W. L. Bragg and J. West, Proc. Roy. Soc. London, Ser. A, 1927, vol. 114, p. 456. [M.A. 3–342.]

those in an octahedral face of gahnite. A relationship between crystal-structures and, therefore, the X-ray photographs of nigerite and gahnite is, of course, to be expected and is well shown by the strong lines on the powder photographs of the two minerals reproduced in

TABLE II. X-ray powder data for nigerite.

2r cm.	Intensity.	Spacing Observed. kX.	Spacing Calculated. kX.	Index.	2r cm.	Intensity.	Spacing Observed. kX.	Spacing Calculated. kX.	Index.
1·91	ms	4·64	4·656	$10\bar{1}1$	6·96	vw	1·348	1·353	$11\bar{2}9$
2·22	m	4·00	4·023	$10\bar{1}2$	7·05	vw	1·333	1·332	$1\cdot0\cdot\bar{1}\cdot10$
2·66	vw	3·35	3·372	$10\bar{1}3$	7·42	m	1·276	1·275	$31\bar{4}4$
3·15	vs	2·83	2·855	$11\bar{2}0$	7·72	w	1·233	1·236	$40\bar{4}0$
			2·834	$10\bar{1}4$				1·231	$40\bar{4}1$
3·71	vs	2·42	2·434	$20\bar{2}1$				1·228	$31\bar{4}5$
			2·427	$11\bar{2}3$	7·85	w	1·216	1·218	$1\cdot0\cdot\bar{1}\cdot11$
4·15	mw	2·17	2·179	$20\bar{2}3$				1·217	$40\bar{4}2$
4·52	m	2·00	2·011	$20\bar{2}4$				1·213	$22\bar{4}6$
4·58	w	1·977	1·987	$11\bar{2}5$	8·04	vw	1·192	1·194	$40\bar{4}3$
4·93	m d	1·843	1·843	$20\bar{2}5$				1·193	$30\bar{3}8$
			1·835	$10\bar{1}7$	8·25	vw	1·167	1·164	$40\bar{4}4$
5·05	w	1·804	1·804	$21\bar{3}2$	8·40	vw	1·150	1·153	$0\cdot0\cdot0\cdot12$
			1·794	$11\bar{2}6$				1·150	$1\cdot1\cdot\bar{2}\cdot11$
5·28	vw	1·731	1·732	$21\bar{3}3$*	8·56	w	1·132	1·131	$32\bar{5}1$
			1·729	0008	8·64	w	1·124	1·124	$30\bar{3}9$
5·58	s	1·644	1·644	$21\bar{3}4$				1·123	$1\cdot0\cdot\bar{1}\cdot12$
5·61	vvw	1·636	1·637	$30\bar{3}1$*	9·10	ms	1·079	1·077	$32\bar{5}4$
			1·632	$10\bar{1}8$	9·40	ms	1·052	1·050	$32\bar{5}5$
5·97	s	1·541	1·543	$20\bar{2}7$	9·49	w	1·044	1·046	$22\bar{4}9$
6·32	vw d	1·469	1·477	$11\bar{2}8$				1·045	$41\bar{5}3$
			1·468	$10\bar{1}9$				1·044	$2\cdot0\cdot\bar{2}\cdot12$
6·51	ms	1·430	1·428	$22\bar{4}0$				1·043	$2\cdot1\cdot\bar{3}\cdot11$
6·60	ms	1·413	1·417	$20\bar{2}8$	9·95	mw	1·008	1·006	$40\bar{4}8$
			1·416	$30\bar{3}5$*	10·06	vw	1·000	1·000	$41\bar{5}5$
6·87	w	1·363	1·358	$21\bar{3}7$				1·000	$3\cdot0\cdot\bar{3}\cdot11$

* Spots corresponding to these indices are either very weak or not observed on a rotation photograph of a single crystal of nigerite about the [0001] axis.

The above data were obtained from an X-ray photograph of powdered nigerite taken with filtered copper radiation λ1·539 kX in a cylindrical camera, 5·73 cm. diameter. Relative intensities are given as: vs very strong, s strong, ms medium strong, m medium, mw medium weak, w weak, vw very weak, vvw very very weak; d, doublet measured as a single line.

fig. 1. Indexed powder data of nigerite are given in table II and the spacings calculated from the unit-cell dimensions are also tabulated. Several lines are unresolved doublets or triplets, and it is possible on the basis of an indexed rotation photograph of a single crystal of nigerite about the *c*-axis [0001] to exclude those planes which yield very weak spots or spots which are too weak to observe. These are asterisked in the table. The X-ray data obtained for Nigerian gahnite *a* 8·09 kX are

in close agreement with those published for gahnite from the Erik Mattsgrufvan, Falun, Sweden, by Sven Holgersson,[1] and with data for artificial $ZnAl_2O_4$ by L. Passerini[2] and by G. L. Clark, A. Ally, and A. E. Badger.[3]

The refractive indices and specific gravities of gahnite range from 1·782 and 4·38 to 1·818 and 4·57,[4] the corresponding values for the artificial compound being 1·805 and 4·55.[5] L. J. Spencer's range of specific gravity for the mineral is 4·478–4·602.[6] Nigerian gahnite has a refractive index very close to 1·80 and sinks in saturated Clerici solution so that its specific gravity is >4·5. It is probable, therefore, that the Nigerian mineral is close in composition to the ideal formula $ZnAl_2O_4$.

[1] S. Holgersson, Lunds Univ. Årsskr., Ny Följd, Avd. 2, 1927, vol. 23, no. 9, p. 31.

[2] L. Passerini, Gazz. Chim. Ital., 1930, vol. 60, p. 394.

[3] G. L. Clark, A. Ally, and A. E. Badger, Amer. Journ. Sci., 1931, ser. 5, vol. 22, p. 541. [M.A. 5–178.]

[4] Dana's System of mineralogy. 7th edit., New York, 1944, p. 691. [M.A. 9–85].

[5] E. S. Larsen and H. Berman, Microscopic determination of the nonopaque minerals. 2nd edit., 1934, p. 58.

[6] L. J. Spencer, Min. Mag., 1927, vol. 21, p. 362.

An interferometric survey of the micas.

(With Plates VII–IX.)

By S. Tolansky, D.Sc., Ph.D., D.I.C., and Pamela G. Morris, M.Sc.
Royal Holloway College, London University.

[Communicated by Dr. G. F. Claringbull; read May 22, 1947.]

Introduction.

In a group of earlier publications[1] details have been given of the application of multiple-beam interference methods to the study of mica. The characteristic structure of this mineral is exhibited by the Fizeau fringes which are produced when one side of a mica slip is silvered and placed against a similarly coated optical flat. The fringes show that the surface is violently contorted and crossed by cleavage steps, the heights of which appear to be integral multiples of the crystal-lattice spacing perpendicular to the basal plane of cleavage. If, however, a mica slip (thickness *circa* 1/100 mm.) is silvered on both sides then fringes of a totally different appearance are observed. It is frequently found that, despite the distortions on the surface, the Fizeau fringes are large *areas* of uniform illumination bounded by cleavage 'lines'. It has already been shown by multiple-beam Fizeau fringes and by the multiple-beam fringes of equal chromatic order that: (1) the contortions on one side are faithfully followed by those on the other to within molecular dimensions; (2) the mica can cleave true to a single molecular lattice over a very extensive area (many square centimetres); (3) inclusions (solid, liquid, or gaseous) which are normally not visible are shown up in detail; (4) variations in chemical composition are revealed; (5) the birefringence is shown over an extensive wave-length range.

In the earlier experiments a few samples of muscovite of unknown origin were studied, and because of its widespread use and ubiquity in rock distribution it seemed desirable to undertake a systematic survey of micas from different regions. For this purpose we have secured from the Mica Control Board twenty-five samples of known origin. These

[1] S. Tolansky, Proc. Roy. Soc. London, Ser. A, 1945, vol. 184, p. 51; ibid., 1946, vol. 186, p. 261; Phil. Mag., 1946, ser. 7, vol. 37, p. 390. [M.A. 10–134.]

micas have been examined by the multiple-beam methods formerly described. They have been graded according to their optical perfection, and at the same time measurements have been made on dielectric power loss, but a report on this technological aspect is not given here. Local structure features have been investigated in some instances.

Description of Materials Examined.

The varieties of mica available comprised 18 muscovites, 4 phlogopites, 2 biotites, and 1 lepidolite. There was a sufficient quantity of each to permit of the examination of many different samples belonging to any group. The micas as received were graded commercially in accordance with the following scheme. In this grading the micas are selected for their optical clarity and freedom from flaws and inclusions when held against a diffuse white light source. Most of the muscovites would be graded as of high quality commercially.

Table I. Mica varieties.

No.		Designation and origin.	General description (white light).
1	Muscovite.	Clear green, Madras	Slightly mottled, feather-like inclusions
2	,,	Clear green, East Africa	Very clear, stained green
3	,,	Dark ruby, East Africa	Very clear, ruby
4	,,	Ruby A.Q., Madras	Clear, surface scratches
5	,,	Clear green, Madras	Pale green, very clear
6	,,	Ruby B.Q., Madras	Clear, mottled, inclusions
7	,,	Ruby C. and S.S., Rhodesia	Very clear, ruby, surface scratches
8	,,	C. and S.S., Brazil	Clear, colourless, very uniform
9	,,	C. and S.S., Tanganyika	Clear
10	,,	C. and S.S., Calcutta	Clear, few inclusions
11	,,	F.S., Rhodesia	Clear, light ruby, surface scratches
12	,,	F.S., Brazil	Clear, few inclusions
13	,,	F.S., Tanganyika	Clear, few stains
14	,,	F.S., Bihar	Clear
15	,,	G.S., Calcutta	Very clear
16	,,	S., Brazil	Clear, slightly mottled, included crystals
17	,,	S., Calcutta	Clear, mottled inclusions
18	,,	Brazil	Clear, mottled
19	Phlogopite	Amber, Madagascar	Transparent, green-brown, stained, slightly mottled
20	,,	Amber, Madagascar	Almost opaque, black, masses of inclusions
21	,,	Dark amber, Travancore	Dark brown, fairly clear, mottled, bubble chains

TABLE I (*continued*)

No.	Designation and origin.	General description (white light).
22	Phlogopite Ontario	Opaque, metallic, buckled lump
23	Biotite —	Black, stained, almost opaque, many bubbles
24	„ —	Black, mottled, 'dusty' appearance, many small bubbles
25	Lepidolite —	Quite clear, brittle and stiff

Abbreviations of gradings kindly supplied by F. F. Chrestian & Co.:

C. & S.S. Clear and slightly stained. F.S. Fair stained. G.S. Good stained. S. Stained. H.S. Heavily stained. D.S. Densely stained. A.Q. First quality. B.Q. Second quality.

The muscovites were all initially selected as of good commercial optical quality and although a number were stained or coloured, all showed large areas which were apparently flawless visually. As shown below, the sensitive multiple-beam methods reveal the existence of inclusions and structures not visible by direct means.

EXPERIMENTAL.

Thin sheets of mica (*circa* 1/100 mm.) were cleaved from the samples supplied and silvered on both sides by evaporation *in vacuo* in accordance with a technique formerly described, with reflecting coefficients sometimes approaching 0·94. As shown elsewhere,[1] with such silverings a multiple-beam Fizeau fringe set-up leads to the formation of uniformly tinted areas when a mercury-arc source is used. A simple calculation shows that a change in thickness of *but a single crystal-lattice layer* (20 Å.U.) can lead to a 50 % change in the intensity, hence adjacent regions which are separated by even only one lattice layer show easily distinguishable areas on the interferogram. The micas were examined with Fizeau fringes employing magnifications varying from $\times 3$ to $\times 200$ and using various isolated and mixed monochromatic radiations from a mercury-arc source. A number of features of special interest were examined with the white-light fringes of equal chromatic order and these reveal local details and birefringence effects.

So complex are the features revealed and so rich is the detail often exhibited even on a single interferogram, that any attempt at a full description of what has been observed would occupy a prohibitive amount of print. We therefore reproduce typical Fizeau fringe interferograms in pl. VII, figs. 1–9, since they are much more revealing than

[1] S. Tolansky, Proc. Physical Soc., 1946, vol. 58, p. 654. [M.A. **10**–134.]

simple descriptions. Explanations of the plates are given at the end of this paper.

It was first proved that any interferogram is indeed typical of a given kind of mica. Each variety, as received, contained a number of fairly thick sheets of material. For a given variety a random selection of a dozen pieces was taken from various sheets. The interferograms were examined, and it was observed without any doubt that the random samples from any one variety closely resembled one another and can all differ distinctly from some other variety. It can be confidently asserted that the reproductions in figs. 1–9 are typical for the varieties indexed.

In three of the photographs secondary fringes of low visibility can be seen within the uniform tint areas. In these cases the mica slips have been mounted between glass plates both to protect the silver from atmospheric attack and to assist manipulation (a freely suspended thin sheet is sensitive to air shocks). These secondaries are formed in the air films between the silvered mica and the unsilvered glass surfaces. They show that although an area is of uniform tint yet the corresponding mica surface is highly distorted, from which it follows that identical distortions occur on both faces of the mica. The secondaries are eliminated when the mica is freely suspended, and for particular investigations this was frequently done.

Discussion of Fizeau Fringes.

The degree of optical uniformity of the various mica samples is shown by the fringes in figs. 1–9 inclusive. As indeed may be expected, the white-light insensitive grading only correlates crudely with this. It will be shown elsewhere that a precision grading can be made on the basis of the interferograms and it has in fact been found possible to derive some correlation between the character of the inclusions and the dielectric power loss. We shall here survey only the general characteristics shown by the interferograms, discussing in particular some specific points of interest, whilst recognizing that we are leaving completely untouched a mass of material already readily available for study on these photographs. In particular we have made estimates of: (1) the average area of uniformity; (2) the largest area of uniformity found for the given variety; (3) inclusions visible per square centimetre. The data are given in table II for all the samples studied. The number of inclusions observed depends, of course, on the volume, but since all the samples selected were roughly 1/100 mm. thick, the visual number

count (being in any case only an approximation) can be taken as a measure of the number of inclusions per cubic centimetre of mica. The figure given is then approximately the number of inclusions per cubic millimetre of mica.

TABLE II (For sheets *circa* 1/100 mm. thick.)

No.	Mica.	Average area of uniformity sq. cm.	Largest uniform area sq. cm.	Inclusions per sq. cm.	Remarks.
1	Muscovite	0·06	1	17	Large network of fine bubbles
2	,,	0·9	14	—	—
3	,,	0·7	6	—	—
4	,,	0·6	5	—	—
5	,,	0·7	6	—	—
6	,,	0·1	1·5	20	Large fluctuations in area
7	,,	0·3	1	—	—
8	,,	0·9	13	—	—
9	,,	0·5	10	1	A few large inclusions
10	,,	0·7	6	2	Non-uniform patchy areas of bubbles
11	,,	1·0	20	—	—
12	,,	0·5	5	1	A few large bubbles
13	,,	1·3	26	—	—
14	,,	1·4	11	—	A few large bubbles
15	,,	0·7	5	11	—
16	,,	0·5	4	4	—
17	,,	0·7	8	7	—
18	,,	0·4	3	3	—
19	Phlogopite	0·06	0·5	15	Dense local patches of inclusions
20	,,	0·01	0·5	200	—
21	,,	0·06	0·5	52	Many pin-point inclusions
22	,,	—	—	200	Many bubbles, boundaries are obscured
23	Biotite	0·11	0·25	55	Ragged areas dotted with bubbles
24	,,	0·1	0·04	100	—
25	Lepidolite	0·45	1	—	—

Muscovites.—Almost without exception the muscovites exhibit considerable regions of uniform tint, areas which are free from inclusions and over which cleavage is probably true to a single molecular lattice.

The white-light visual commercial grading is only a rough index. Thus, to select but one instance, whilst no. 3 is clearly of high quality, no. 8 is equally good and both are much better than no. 1.

On the basis of these observations the micas can be regraded into the following order in which the samples are tabulated in accordance with the value of the *average* of the area of uniformity, the first in the list having the largest *average*, namely, 1·4 square centimetres: nos. 14, 13, 11, 2, 8, 3, 5, 10, 17, 15, 4, 12, 9, 16, 18, 7, 6, 1. As seen, since the commercial grading is in sequence 1, 2, 3, 4 . . . 18, correlation is virtually non-existent within the muscovite group, nor does grading according to the number of inclusions offer a better correlation. Clearly the commercial grading is inadequate.

Of striking crystallographic interest is the fact that certain of the muscovites exhibit relatively enormous areas which have cleaved true to a single molecule *on both sides of the sheet*. The largest single area we have observed is 26 square centimetres and over such extensive regions it must be considered that one has true perfect cleavages on either side of a single crystal. Since such mica sheets are clearly ideal for functioning as α-particle absorbing screens, windows, &c., we list below in order of merit the four varieties which we have found the best from this point of view.

TABLE III. Muscovites with large uniform areas.

No.	Origin.	Average uniform area (sq. cm.).	Largest uniform area (sq. cm.).
13	F.S., Tanganyika	1·3	26
11	F.S., Rhodesia	1·0	20
2	Clear green, East Africa	0·9	14
8	C. & S.S., Brazil	0·9	13

Figs. 2 and 5 are samples of specimens whose Fizeau fringes show good uniform tint areas. Fig. 2 is shown here with strongly developed secondaries to illustrate the nature of these, whilst in fig. 5 the mica is freely suspended.

Phlogopites.—The phlogopites examined, although from widely different geographical regions, show interferograms resembling one another and all totally distinct from the typical muscovites. Extensive areas of uniform tint are absent, the specimens often consisting of a confused mass of small elements. The number of inclusions is considerable and several samples exhibit more than 200 inclusions per cubic millimetre. It is clear that the natural phlogopites are less perfect crystals than are the muscovites.

It may be noted that one particular phlogopite (a light variety of Travancore amber) showed a few moderately large uniform tint areas (one of 4 sq. cm.) and this is possibly a phlogopite showing some muscovite interpenetration.

Biotites.—The two biotites examined do not differ much in appearance from the phlogopites.

Lepidolite.—One good-quality lepidolite sample was available. The interferogram somewhat resembled a muscovite and showed that the crystal was chemically extremely homogeneous although the areas of uniform thickness were comparatively small.

Some Specific Features.

From amongst the considerable detail presented we have selected some features of interest for discussion.

(1) *Bubble Chains.*—Chains of bubbles have been found on at least four muscovites, two phlogopites, and one biotite, appearing therefore to be ubiquitous in micas; pl. VII, fig. 7 shows a typical example. A portion of the same chain with higher magnification is shown in pl. VIII fig. 12. It can be seen that the chain consists of a series of discrete ellipsoidal bubbles. The curvature is so high that the fringe localization in the mica film no longer exists. Hence the fringes within the bubbles are completely out of focus and thus abnormally broad.

(2) *Filament Channels.*—The origin of these bubble chains is possibly associated with the detail shown in fig. 11 ($\times 51$) which is from a muscovite. This is a filament channel, probably liquid and about 0·03 mm. wide, which is just about the width of a typical bubble chain. Clearly such a liquid channel could break up into a bubble chain through continued crystal growth into the channel.

Similar channel-like markings are common features on other samples; fig. 4 is an example. Some of these filaments are almost in the stage of breaking up, and some are so fine as to give interference colours in white light.

(3) *Crystalline Inclusions and Bubbles.*—Crystalline inclusions in mica are, of course, well known. We illustrate in fig. 10 (magnification $\times 42$, insets $\times 230$ approximately) several particularly well-marked crystal plates (A and B) which are clearly visible with the increased contrast produced by multiple-beam interference. The visibility has been further enhanced for the small details by using a high-pressure mercury-arc source. This increases the fringe width and reduces the risk of the fringe maximum missing the detail under observation. In

many mica specimens inclusions of the nature of 'dust' are observed. As in the upper part of fig. 10 these are often too small for structure detail to be resolved. We cannot give any information concerning the chemical nature of the inclusions.

Regarding the character of the many bubble-like inclusions observed, little can be said. It is probable that the nearly circular inclusions (as in pl. IX, fig. 14) are liquid. In some cases crystalline material appears to be present, whilst other bubbles are so perfectly circular that they almost certainly consist of liquid drops held under high surface tension forces.

Many curious effects have been noted. Pl. VIII, fig. 13 shows the Fizeau fringes produced when one bubble lies beneath another, and similar confused fringes can always be seen in biotites.

(4) *Birefringence.*—It has already been shown that the birefringence of mica in the direction perpendicular to the cleavage plane can be demonstrated over an extensive wave-length range with white-light fringes of equal chromatic order. We show in pl. IX, figs. 16, 17, 18 a series of such fringes for different specimens which are optically biaxial. The fringe doubling $d\lambda$ is related to the birefringence $d\mu$ by the simple expression $d\lambda = (\lambda/\mu) \cdot d\mu$. This is independent of the thickness of the mica sheet used, and these fringes could be used to convert easily measured $d\lambda$ values into absolute values of $d\mu$. However, our use for the fringes has been to demonstrate differences in cleavage quality. Those micas (as in figs. 2 and 5) which give Fizeau fringes over large areas have smooth straight fringes of equal chromatic order (fig. 16). Other types show highly ragged broken fringes, as in figs. 17 and 18.

Explanation of Plates VII–IX.

Plate VII. Fizeau fringes of doubly silvered mica sheets.

Fig. 1. Muscovite, green, Madras (specimen 1). A number of small inclusions. ×55.

Fig. 2. Muscovite, ruby, Madras (specimen 6). Uniform tint areas crossed with low-visibility secondary fringes. ×24.

Fig. 3. Muscovite, Bihar (specimen 14). Large uniform tint areas. Inclusion showing fringe doubling due to birefringence. ×7.

Fig. 4. Muscovite, Calcutta (specimen 15). Showing bubble chains. ×55.

Fig. 5. Muscovite, Brazil (specimen 18). Areas of high uniformity. ×51.

Fig. 6. Phlogopite, amber, Madagascar (specimen 20). Numerous inclusions. ×31.

Fig. 7. Phlogopite, light amber, Travancore (specimen 21). Inclusions and series of bubble chains. ×55.

FIG. 8. Phlogopite, dark amber, Travancore (specimen 21). Large inclusion. Does not exhibit birefringence doubling. ×55.

FIG. 9. Biotite (specimen 24). Many irregular inclusions. ×51.

PLATE VIII. Fizeau fringes of doubly silvered mica sheets.

FIG. 10. Phlogopite, dark amber, Travancore (specimen 21). Showing large inclusion. ×42. Inset A (×230) enlarged portion showing crystal inclusion. Inset B (×230) enlarged portion showing crystal plate inclusion and 'dust'-like specks of included matter.

FIG. 11. Muscovite, Calcutta (specimen 15). Showing filament channel. ×51.

FIG. 12. Phlogopite, light amber, Travancore (specimen 21). Showing enlarged detail of bubble chains as ellipsoidal features. ×83.

FIG. 13. Phlogopite, dark amber Travancore (specimen 2). Overlapping inclusions. ×130.

PLATE IX, FIGS. 14, 15. Fizeau fringes of doubly silvered mica sheets.

FIG. 14. Biotite (specimen 23). The circular rings suggest liquid inclusions. ×40.

FIG. 15. Muscovite, Bihar, F.S. (specimen 14). Large bubble-like inclusion, showing birefringence effect and also crystal-like nucleus. ×15.

FIGS. 16, 17, 18. Fringes of equal chromatic order for three different muscovites, showing differences in cleavage behaviour. The fringes are double because of birefringence. Fig. 16 is the type of fringe given by the majority of the muscovites.

An interferometric examination of synthetic mica.

(With Plate X.)

By S. Tolansky, D.Sc., Ph.D., D.I.C., and Pamela G. Morris, M.Sc.

Royal Holloway College, London University.

[Communicated by Dr. G. F. Claringbull; read May 22, 1947.]

Introduction.

A RECENT report[1] has appeared describing a process developed in Germany for the production of a crystal described as synthetic mica. The details are given for a process used at Ostheim and reference is also made to a Siemens–Halske technique. Through the courtesy of Mr. Kendall of Metropolitan-Vickers we have secured a few small samples of the Siemens–Halske material. This is reported to be a fluor-phlogopite with the chemical composition $KMg_3AlSi_3O_{10}F_2$ and free from water of constitution. Claims made by the manufacturers stated that the synthetic material exhibits the cleavage characteristics of natural mica.

The few samples we have obtained have areas somewhat less than a square centimetre and we have selected thin cleavage flakes and submitted them to interferometric examination with the multiple-beam technique. Since we have already studied 25 natural micas (see preceding paper), the main purpose of this note is to report upon both how closely the synthetic material mimics the natural mineral and upon any differences. For this purpose use has been made of multiple-beam Fizeau fringes using a mercury-arc source, with both filtered and mixed radiations. Although described as a phlogopite the material is quite colour-free (presumably due to the absence of iron), highly transparent, and visually resembling a high-grade muscovite rather than the mineral phlogopite.

Experimental.

(*a*) *Surface topography.*—Thin flakes (*circa* 1/100 mm. thick) were cleaved off, the mechanical act of cleavage closely resembling that of the

[1] A. E. Link, Investigation of a synthetic mica process, Ostheim, Germany. Combined Intelligence Objective Sub-committee, no. 22, xxii–11, London (H.M. Stationery Office), 1945. [M.A. **10**–108.]

natural micas. The thin sheets were silvered on one side and matched close against a high-grade silvered optical flat. The Fizeau fringes so formed for a cleavage surface closely resemble the typical fringes given by a natural mica, examples being shown in pl. X, figs. 1–3 (green mercury-line source). The smooth continuity of the fringes (fig. 1) is typical of mica and the cleavage steps quite characteristic. There is, however, a notable distinction in some regions. In practically every natural mica examined the value of the cleavage step remains constant to within the limit of observation along the length of the step, i.e. the surfaces above and below the step are 'parallel'. On the synthetic crystal, however, adjacent surfaces on either side of some cleavage lines are inclined to each other. In one case, for example, the angle of slope is $2\frac{1}{2}$ minutes of arc. Interferometrically this is a considerable angle, since a slope of only 1/250th of this amount can readily be detected even over only a 1 mm. length of crystal. The implications of this difference will be discussed later.

(*b*) *Doubly silvered film.*—The thin films were examined by silvering both sides and viewing the Fizeau fringes formed *within* the body of the crystal. Typical examples taken with monochromatic radiation are shown in pl. X, figs. 4–6.

Interpretation.

When these interferograms are compared with those of the natural mineral micas illustrated in the previous communication, four features emerge:

(1) The synthetic material clearly has a polycrystalline nature, whilst the natural micas tend to grow in large plates.

(2) The synthetic material shows comparatively few enclosed bubbles or gas pockets and in this respect is greatly superior to the natural phlogopite.

(3) Whilst natural mica cleaves in 'parallel' steps, such that a sheet is built up of regions which are of different thickness yet have strictly parallel faces, there are, on the other hand, frequent 'wedge' fringes in the synthetic sheet. An exaggerated schematic diagram illustrating the effect is shown in text-fig. 1. In this diagram the buckling and distortion of the sheet is disregarded. *A* shows the parallel-sided cleavage of the natural mica; and *B* the 'wedge' formation of the synthetic material, with gross exaggeration of the wedge angles which are only of the order of a few minutes of arc at most. This type of structure accounts for the observations made on both singly and doubly silvered specimens.

There seems no doubt that this illustrates a marked distinction between the natural and synthetic materials. All the evidence so far found shows that large natural mica crystals grow in strictly *parallel* sheets. The synthetic material appears to consist of a conglomeration of crystals which are *almost* but not quite parallel in many regions. The deviation from parallelism varies considerably from region to region.

(4) *Birefringence fringe doubling.*—Phlogopites do not show birefringence doubling of fringes, and indeed this is what we have found over

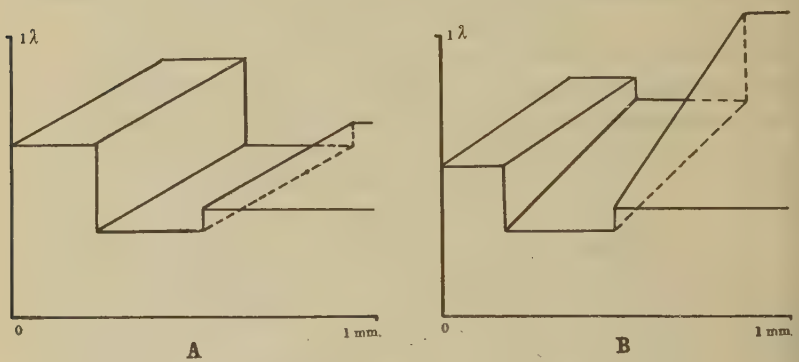

TEXT-FIG. 1. Diagram of cleavage surfaces. A, natural mica; B, synthetic mica.

practically the whole of the synthetic material. On one sample, however, there was a region which cleaved to give uniform tint areas over an appreciable area, a characteristic shown usually by the muscovites. In this local region the synthetic material showed a birefringence effect of the muscovite type, and, locally, either some intermediate crystal type has formed or some kind of twinning exists. Only a small fraction of the total area examined showed this complexity.

Disintegration of the silver film.

A notable difference between the natural and synthetic materials is shown by the fact that the cleaved surface of the synthetic crystal is chemically active and rapidly disintegrates the silver surface. On the other hand, on practically all the natural micas the silver surface remains stable over many months. (In rare instances local disintegration sets in over very small regions. This will be discussed elsewhere.)

The disintegration is shown in pl. X, figs. 7 and 8, which represent monochromatic Fizeau fringes of a doubly silvered slip of the synthetic material taken respectively one week and ten days after silver deposition.

It can be seen that over the whole surface area small nuclei act as disintegrating centres, and the silver is destroyed in circular patches spreading out from each nucleus. The successive stages of the break-up can be clearly followed in the interferograms. Such material can clearly not be used as a silvered mica condenser.

It is clear that the synthetic material is an imperfect crystal. The destruction of the silver is obviously chemical and may be due possibly to fluorinated centres, or some other chemically active constituents. We have occasionally witnessed the break-up of silver films when deposited on dirty surfaces, but such break-up is rarely as violent as that shown here. The cleavage face of the crystal was free from extraneous dirt and impurity, but may easily have contained unconverted particles of the constituent mother materials from which the crystal was made. The amount of silver involved in the large disk in fig. 8 is only 3×10^{-8} gram.

Summary.

(1) The synthetic material is highly transparent and contains few inclusions.

(2) Cleavage closely approximates to that of a natural mica, but differs in detail.

(3) The material appears to be largely polycrystalline consisting in parts of almost parallel plates.

(4) As distinct from the natural mica the synthetic material has numerous chemically active centres which attack silver.

(5) Most of the material shows no birefringence on the cleavage surfaces, but a local birefringent area has been found.

It may be concluded that the synthetic material is much more free from inclusions than natural phlogopite. In this respect it closely resembles a muscovite. Crystallographically, however, it is less perfectly formed than a natural mica, although the differences as listed above are not such as to make a serious distinction. In cleavage and structural characteristics, as in homogeneity, the synthetic material is inferior to a good grade of muscovite, but superior to a natural phlogopite.

Explanation of Plate X.

Synthetic mica (fluor-phlogopite).

Figs. 1–3. Fizeau fringes of single cleavage faces.

Fig. 1. Shows smooth continuity of fringes. This region resembles the surface of a muscovite. ×30.

Fig. 2. Typical cleavage step. ×30.

Fig. 3. Typical of natural mica, showing numerous cleavages, but some surface irregularity. In some cases the fringes separated by a cleavage get out of step, indicating a wedge. ×30.

Figs. 4–6. Fizeau fringes of doubly silvered sheets.

Fig. 4. The uniform tint areas resemble those of muscovites. In contradistinction to natural phlogopite there is a notable absence of inclusions. ×30.

Fig. 5. Showing irregular internal wedges. ×30.

Fig. 6. Showing a section exhibiting wedge fringes, indicating the two faces of the mica sheet are not quite parallel. ×30.

Figs. 7 and 8. Fizeau fringes illustrating the chemical destruction and disintegration of the silver film on synthetic mica, increasing progressively with age.

Fig. 7. Surface after 7 days, originally as clear as in fig. 4. ×36.

Fig. 8. Same surface as in fig. 7 three days later. Surface breaks up by spread of circular rings of opacity. ×36.

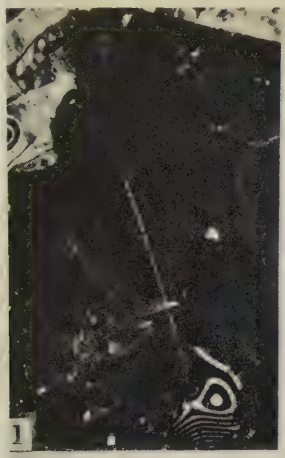

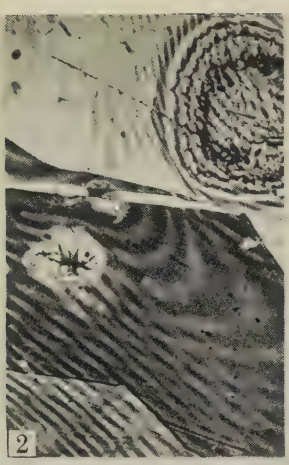

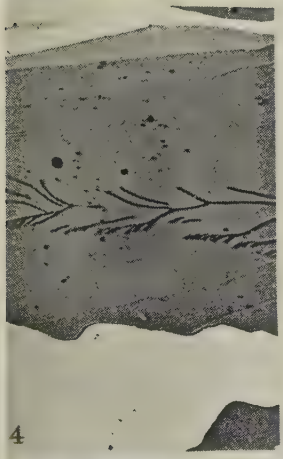

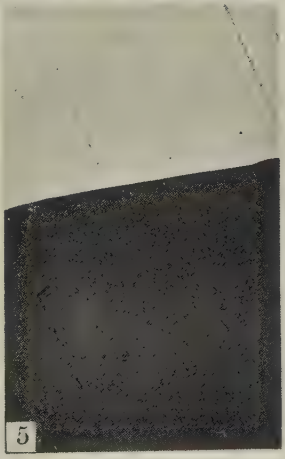

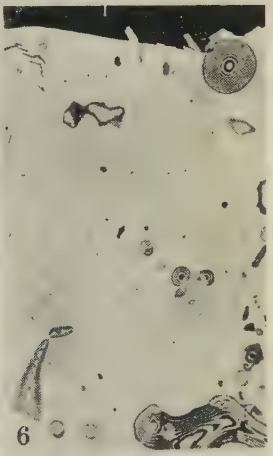

S. Tolansky and P. G. Morris: Interferometry of Micas.

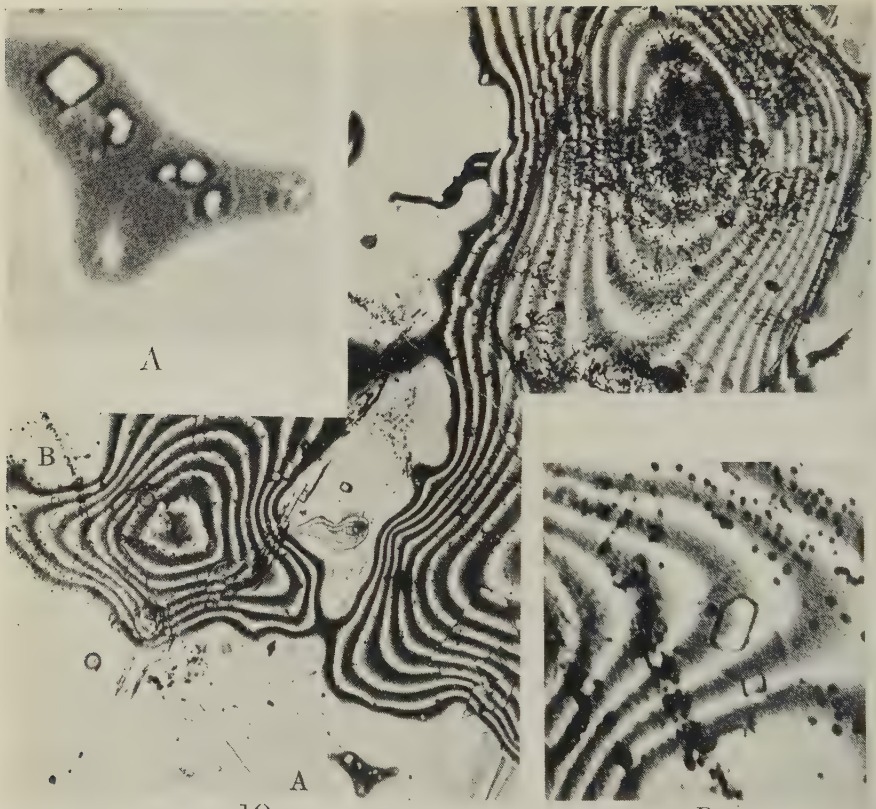

10

B

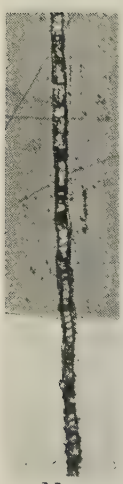

11

12

13

S. TOLANSKY AND P. G. MORRIS: INTERFEROMETRY OF MICAS.

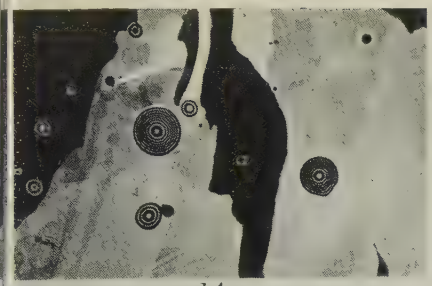

14

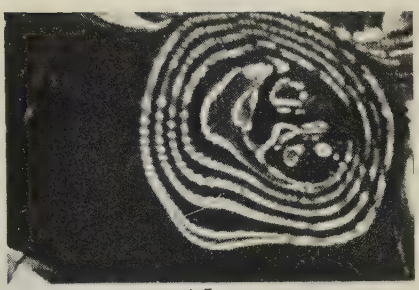

15

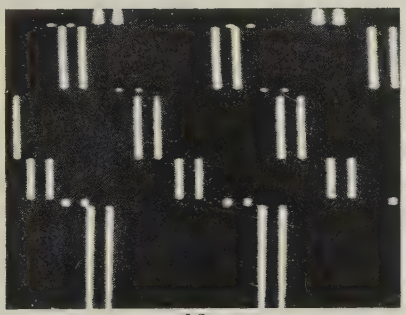

16

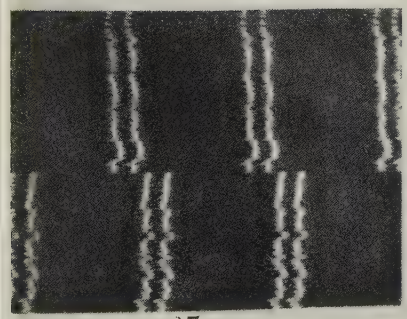

17

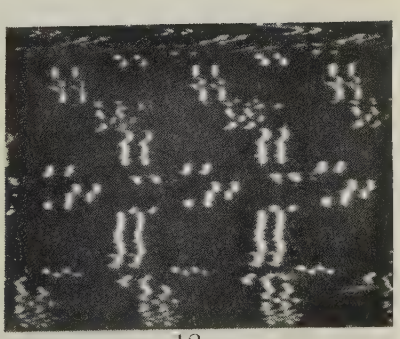

18

S. Tolansky and P. G. Morris: Interferometry of Micas.

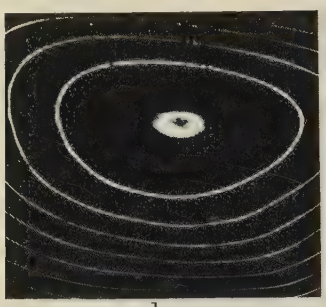

1

2

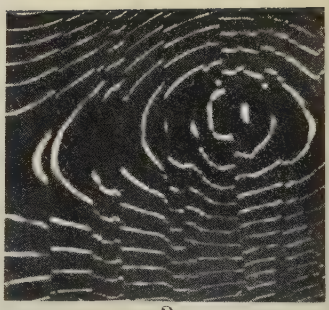

3

4

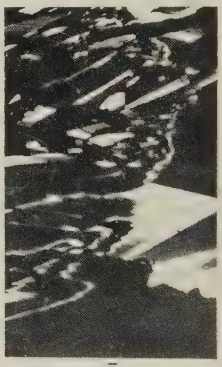

5

6

7

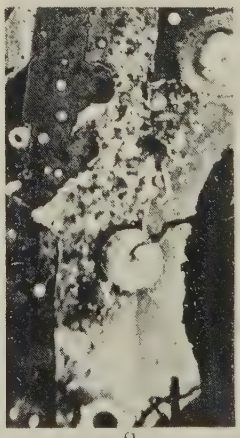

8

S. TOLANSKY AND P. G. MORRIS: INTERFEROMETRY OF SYNTHETIC MICA.

On tilleyite and its associated minerals from Carlingford, Ireland.

(With Plates XI and XII.)

By S. R. Nockolds, Ph.D., F.G.S.

With chemical analyses by H. G. C. Vincent, M.A.

Department of Mineralogy and Petrology, University of Cambridge.

[Read March 27, 1947.]

THE mineral tilleyite was first discovered by Larsen and Dunham in thermally metamorphosed limestones from the contact zone at Crestmore, California.[1] It is associated there with merwinite, wollastonite, spurrite, and gehlenite, and the rock is traversed by streaks of idocrase with grossular. The amount of tilleyite in these rocks was apparently small, but in certain thermally metamorphosed limestones from Carlingford it is abundant and some specimens are practically pure tilleyite-rocks. It has been possible, therefore, to make a more detailed optical and chemical examination of this mineral. The tilleyite occurs as subidioblastic crystals when abundant, or as rounded grains in calcite-rich rocks, or as irregular plates.

(a) *Optical properties of tilleyite.*

According to Larsen and Dunham tilleyite is monoclinic with one perfect cleavage, assumed to be parallel to (100), and with traces of another ill-defined cleavage which makes an angle of about 42° with the perfect cleavage. The β index direction was found to be in the plane of the perfect cleavage, i.e. $\beta = b$. The α index direction was said to make an angle of 18° with the trace of the perfect cleavage in a section parallel to (010). The refractive indices were determined as α 1·617, β 1·635, γ 1·652, while 2V was found to be large, approaching 90°, and probably positive. Twinning was not detected.

These results are confirmed in part by an examination of the Carlingford tilleyite, but several cleavages have been found in addition to the

[1] E. S. Larsen and K. C. Dunham, Tilleyite, a new mineral from the contact zone at Crestmore, California. Amer. Min., 1933, vol. 18, pp. 469–473. [M.A. 5–387.]

perfect one. Simple or, more rarely, lamellar twinning is common (pl. XI, figs. 1 and 2), and the optical orientation is different. The refractive indices of the Carlingford material were determined by means of the immersion method; and the optical orientation, optical axial angle, position of the cleavages and of the composition-plane of the

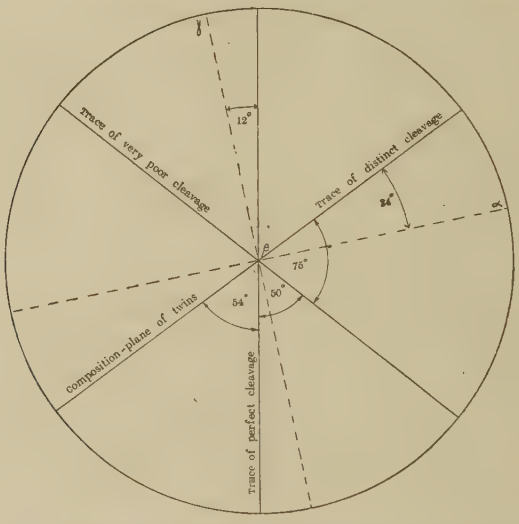

Text-fig. 1. Stereographic projection of tilleyite on a plane normal to $\beta = b$, showing the relations between the cleavages and the optical orientation.

twin-lamellae, by means of the Fedorov universal stage. The results may be summarized as follows:

α 1·612, β 1·632, γ 1·653 (all $\pm$0·003), positive, 2V ranges 85—89° with an average value of 87°.

The optical orientation is shown in text-fig. 1, where the plane of projection is normal to $\beta = b$, that is, the (010) plane if we accept Larsen and Dunham's orientation. In addition to the perfect cleavage parallel to (100), there is a distinct cleavage at right angles to (010) and making an angle of 54° with the perfect cleavage, a poor cleavage parallel to (010), and a very poor cleavage at right angles to (010) making an angle of 50° with the perfect cleavage and of 75° with the distinct cleavage. The composition-plane of the twins coincides with the plane of the distinct cleavage and, in sections normal to β and to the composition-plane, the symmetrical extinction angle (α to trace of composition-plane) is 24°. It will be noticed that the optical orientation

is not the same as that given by Larsen and Dunham. It is the *slow* vibration direction γ which lies near the trace of the perfect cleavage and the angle it makes with the latter is 12° and not 18°. This has been confirmed by an examination of such Crestmore material as is available in the Department of Mineralogy and Petrology, Cambridge.[1]

(b) *Chemical composition of tilleyite.*

Larsen and Dunham managed to separate a small quantity of tilleyite for chemical analysis, but the analysed powder contained a little wollastonite and spurrite. After correcting for the estimated amount of impurity and recalculating the principal constituents to 100%, they obtained molecular ratios suggesting an empirical formula $3CaO.SiO_2.CO_2$, though not agreeing very closely with the theoretical molecular proportions derived from the latter. They conclude, 'Examination of other possible formulae showed that only a very complex one would fit the analysis better than the one assigned, and we have decided, pending the availability of purer material for analytical purposes, to present the formula in its simple form' (loc. cit., p. 472).

There is thus some element of doubt as to the true composition of tilleyite and, in an effort to resolve the problem, two samples of tilleyite were separated from their parent rocks and chemically analysed by Mr. H. G. C. Vincent with the following results:

	1.	2.	1a.	2a.	3a.	1b.	2b.	3b.
SiO_2	24·48	23·72	24·96	24·16	24·66	0·414	0·401	0·409
Al_2O_3, &c. ...	0·42	0·64	—	—	—	—	—	—
Fe_2O_3... ...	0·40		—	—	—	—	—	—
MgO	—	0·03	—	—	—	—	—	—
CaO	55·51	55·79	56·61	56·82	57·34	1·010	1·013	1·023
CO_2	18·07	18·68	18·43	19·02	18·00	0·419	0·432	0·409
$H_2O+110°$ ...	1·26	1·16	—	—	—	—	—	—
$H_2O-110°$ ...	0·30		—	—	—	—	—	—
	100·44	100·02	100·00	100·00	100·00			

1. Tilleyite, tilleyite-rock with accessory wollastonite and idocrase, locality 1, Barnavave, Carlingford. (Weight of sample 0·8 gm.)

2. Tilleyite, tilleyite-calcite-rock with minor idocrase, locality 1, Barnavave, Carlingford. (Weight of sample 0·3 gm.)

1a. Analysis 1 recalculated to 100% ignoring Al_2O_3, &c., and H_2O.

2a. Analysis 2 recalculated to 100% ignoring Al_2O_3, &c., and H_2O.

3a. Theoretical percentage weights for an empirical formula $3CaO.2SiO_2.2CaCO_3$.

1b–3b. Molecular ratios for 1a–3a.

[1] Prof. Tilley has also found this orientation in tilleyite occurring in metamorphosed limestones from the Island of Muck. C. E. Tilley, The gabbro-limestone contact zone of Camas Mòr, Muck, Inverness-shire. Bull. Comm. Géol. Finlande (Eskola volume), 1947 (in press).

Unfortunately tilleyite is a mineral that alters very readily and although separated in a pure state it was not free from traces of alteration. The first sample showed slight alteration to calcite and hillebrandite along the cleavage planes of the grains, while in the second sample a number of the grains were turbid, probably through the development of minute granules of secondary carbonate. If these facts are taken into account, the agreement of both the analyses with the theoretical percentage weights for an empirical formula $3CaO.2SiO_2.2CaCO_3$ must be considered as good, and there can be little doubt that perfectly fresh tilleyite has this empirical composition. Tilleyite is thus related to rankinite in much the same way as spurrite is to larnite:

larnite	Ca_2SiO_4	spurrite ...	$2Ca_2SiO_4.CaCO_3$
rankinite	$Ca_3Si_2O_7$	tilleyite ...	$Ca_3Si_2O_7.2CaCO_3$

(c) *Paragenesis of tilleyite in the thermally metamorphosed limestones of the Carlingford district.*

The following assemblages containing tilleyite have been found:

1. Tilleyite (with minor idocrase and wollastonite).
2. Tilleyite—calcite (with minor idocrase, wollastonite, melilite).
3. Tilleyite—calcite—idocrase.
4. Tilleyite—idocrase (with minor spurrite).
5. Tilleyite—idocrase—wollastonite.
6. Tilleyite—idocrase—spurrite.
7. Tilleyite—spurrite (with minor idocrase).
8. Tilleyite—spurrite—calcite (with minor idocrase and melilite).
9. Tilleyite—melilite—calcite.

These are found interbanded with other assemblages at localities 1 and 2 (see sketch-map, text-fig. 2). Both of these are small patches of limestone resting on the eucrite of the district. Before describing the characters of the minerals associated with tilleyite, it will be convenient to deal with the other high-temperature assemblages.

(d) *Other high-temperature assemblages from the thermally metamorphosed limestones of the Carlingford district.*

A number of other high-temperature assemblages are found interbanded with the tilleyite-bearing rocks at localities 1 and 2:

1. Spurrite—calcite.
2. Spurrite—calcite—idocrase.
3. Spurrite—calcite—wollastonite.
4. Spurrite—wollastonite—idocrase.

5. Spurrite—idocrase (with minor tilleyite and melilite).
6. Wollastonite—idocrase.
7. Wollastonite—idocrase—melilite.
8. Wollastonite—melilite.
9. Melilite—calcite (minor idocrase and wollastonite).
10. Melilite—calcite—idocrase.
11. Melilite (with minor calcite).

The metamorphosed limestones from localities 3 to 7 inclusive (see sketch-map, text-fig. 2) do not contain either tilleyite or spurrite, but a number are rich in melilite. Certain new assemblages are found there, in addition to those already recorded:

1. Melilite—wollastonite—calcite.
2. Melilite—wollastonite—calcite—augite.
3. Melilite—augite.
4. Melilite—wollastonite—augite.
5. Melilite—wollastonite—garnet (±calcite).
6. Melilite—wollastonite.
7. Wollastonite—augite.
8. Wollastonite (accessory augite).
9. Augite—calcite (±melilite).
10. Monticellite—calcite (phlogopite).
11. Forsterite—calcite (spinel).
12. Forsterite—brucite (after periclase) (spinel).

(e) *Description of the minerals.*

Spurrite is very common in a number of the specimens from localities 1 and 2, and, like tilleyite, is colourless in thin sections. It may be distinguished from the latter by its higher refractive indices and by its small negative optic axial angle. The optical data obtained from the spurrite in these Carlingford rocks are: α 1·641, β 1·676, γ 1·681 (all ±0·003), negative, 2V 38°.

It occurs as subidioblastic or rounded grains, also as irregular plates. When found with tilleyite, the latter is normally less idioblastic and may enclose the spurrite grains, while in one or two cases these minerals were intimately intergrown. This may indicate that tilleyite is replacing spurrite in rocks where they occur together, but no conclusive evidence of this was found.

Wollastonite usually forms subidioblastic crystals but may be more or less granoblastic in fine-grained rocks where it is abundant, or may form semi-poikiloblastic plates as, for instance, in some of the rocks rich in melilite. In certain bands composed almost exclusively of wollastonite, this mineral may appear as crystals half an inch or more long. It is a

variety practically free from iron with α 1·620, β 1·631, γ 1·635 (all $\pm$0·003), negative, 2V 38·5°.

Some of the metamorphosed limestones containing tilleyite, spurrite, and wollastonite have been much affected by later retrograde changes. Associated minerals such as idocrase and grossular remain unchanged, but these three are replaced by calcite and varying amounts of a mineral which has all the properties of *hillebrandite* (pl. XII, fig. 2). This occurs as colourless fibrous aggregates and has α 1·607, γ 1·614 (both $\pm$0·003), positive elongation, straight extinction, negative, 2V 51°. Certain sections show anomalous ultra-blue interference colours between crossed nicols. It compares closely with the type material from Velardeña, Durango, Mexico.[1]

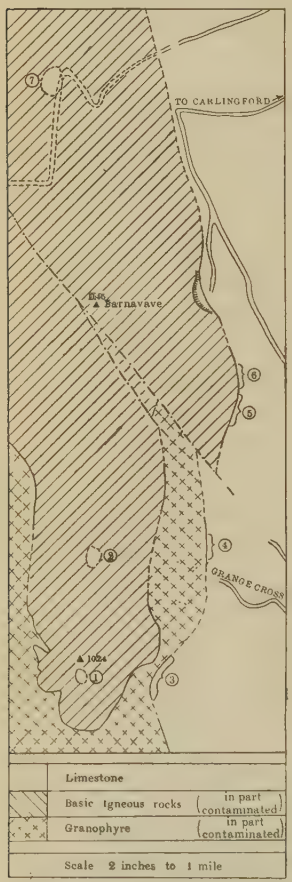

TEXT-FIG. 2. Sketch-map of Barnavave and its surroundings, showing the positions of localities mentioned in the text.

Idocrase is present as a subordinate constituent in many of the assemblages and is sometimes important. It usually builds well-formed idioblastic crystals (pl. XI, fig. 3), though it may be present as more irregular fine-grained aggregates intergrown with wollastonite or melilite. In every example tested it was optically negative with ω 1·726 and ϵ 1·723 (both $\pm$0·003).

Melilite is found as a subordinate constituent in rocks carrying spurrite and tilleyite where it forms small, rather rounded grains. In certain bands interbedded with these rocks and throughout considerable thicknesses of rock at other localities, it becomes abundant and quite a large number of specimens are practically pure melilite-rocks. Under these conditions, the melilite is almost idioblastic and some of the rocks are coarse grained.

This melilite varies somewhat in composition from band to band as is

[1] F. E. Wright, Amer. Journ. Sci., 1908, ser. 4, vol. 26, p. 545.

shown by its optical properties. Some is optically negative with ω 1·650, ϵ 1·648, and shows abnormal ultra-blue colours between crossed nicols; some is isotropic with $\omega = \epsilon$ 1·647; and some is optically positive with ω 1·641, ϵ 1·645, and shows abnormal ultra-brown colours between crossed nicols. In one rock, the melilite was zoned with negative cores and positive margins. It is clear that these melilites contain a considerable amount of the åkermanite molecule, but some of the melilite associated with spurrite and tilleyite in the more calcitic rocks is negative with normal interference colours and must show a closer approach to gehlenite.

Melilite may suffer later alteration and is then converted to a turbid brownish aggregate which is practically isotropic and whose nature could not be further resolved.

The *augite* present in a number of the assemblages from localities 3 to 7 varies from a pale green or colourless diopsidic variety to a pink, somewhat pleochroic titanaugite. The latter is confined to assemblages carrying melilite and is not normally an abundant constituent.

Monticellite, *forsterite*, and *brucite* (forming pseudomorphs after periclase) are confined to rocks occurring at locality 3. These have been described in detail by Osborne (p. 217)[1] together with the phlogopite, pleonaste, apatite, and custerite which accompany the monticellite and also occur in the melilite rocks. The 'vesuvianite' mentioned in Osborne's account of the rocks at this locality is melilite.

Although *custerite*[2] is most abundant in these rocks from locality 3, it is not confined to them. It has been found in small amounts in a spurrite-calcite-rock from locality 1 and more abundantly in some of the melilite-bearing rocks from localities 4, 6, and 7.

The most important accessory constituents are *garnet*, *iron-ore*, and *spinel*, all of which appear in practically every rock examined. The garnet is usually grossular, yellow-green in thin sections, forming small irregular grains enclosed in the main constituents. Occasionally, as in certain melilite-bearing assemblages at locality 6, the garnet is brown in thin sections and must contain an appreciable amount of the andradite molecule. In a melilite-rock at this locality the garnet is poikiloblastic and wrapped round the melilite crystals (pl. XII, fig. 1). Iron-ore is never very abundant, but rarely absent; most of it appears to be

[1] G. D. Osborne, The metamorphic limestones and associated contaminated igneous rocks of the Carlingford district, Co. Louth. Geol. Mag., 1932, vol. 69, pp. 209–233. [M.A. 5–134.]

[2] 'Custerite' = cuspidine, C. E. Tilley, Min. Mag., 1947, vol. 28, p. 91.

pyrrhotine. Spinel is present in varying amounts and tends to be most abundant in the melilite-rich assemblages. It is usually brown in thin sections except in the forsterite-bearing rocks of locality 3 where it is practically colourless.

(f) *The position of tilleyite in the decarbonation series of N. L. Bowen.*

Bowen has dealt recently with the progressive metamorphism of siliceous limestone[1] and has suggested that, after the formation of wollastonite, the next step (at a higher temperature) is the formation of spurrite according to the following equation:

$$3CaCO_3+2CaSiO_3 \rightleftharpoons 2Ca_2SiO_4.CaCO_3+2CO_2.$$

In view of the new data on the chemical composition and occurrence of tilleyite, it seems likely that the formation of this mineral represents an intermediate step between the formation of wollastonite and spurrite:

$$3CaCO_3+2CaSiO_3 \rightleftharpoons Ca_3Si_2O_7.2CaCO_3+CO_2,$$

followed by the reaction:

$$Ca_3Si_2O_7.2CaCO_3 \rightleftharpoons 2Ca_2SiO_4.CaCO_3+CO_2.$$

Explanation of the Plates XI and XII.

Plate XI.

Fig. 1. Tilleyite with simple twinning, tilleyite-rock, locality 1, Barnavave. Crossed nicols. ×25.

Fig. 2. Tilleyite with repeated twinning, spurrite-tilleyite-calcite-rock, locality 2, Barnavave. Crossed nicols. ×25.

Fig. 3. Idioblastic idocrase in spurrite-wollastonite-idocrase-rock, locality 2, Barnavave. Ordinary light. ×25.

Plate XII.

Fig. 1. Poikiloblastic grossular in melilite-rock, locality 6, Barnavave. Ordinary light. ×25.

Fig. 2. Tufted aggregates of hillebrandite with calcite; altered tilleyite-spurrite-calcite-rock, locality 1, Barnavave. Ordinary light. ×32.

[1] N. L. Bowen, Progressive metamorphism of siliceous limestone and dolomite. Journ. Geol. Chicago, 1940, vol. 48, pp. 225–274. [M.A. 8–243.]

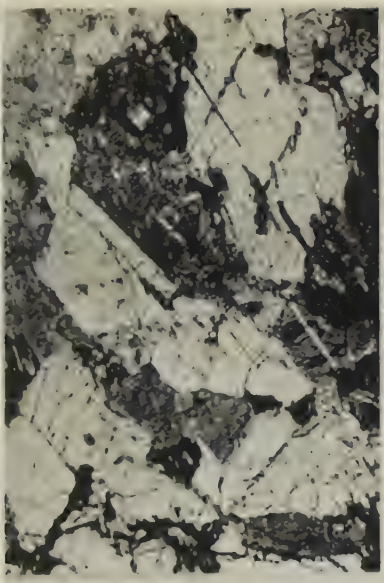

1

2

3

S. R. Nockolds: Tilleyite, etc., Ireland.

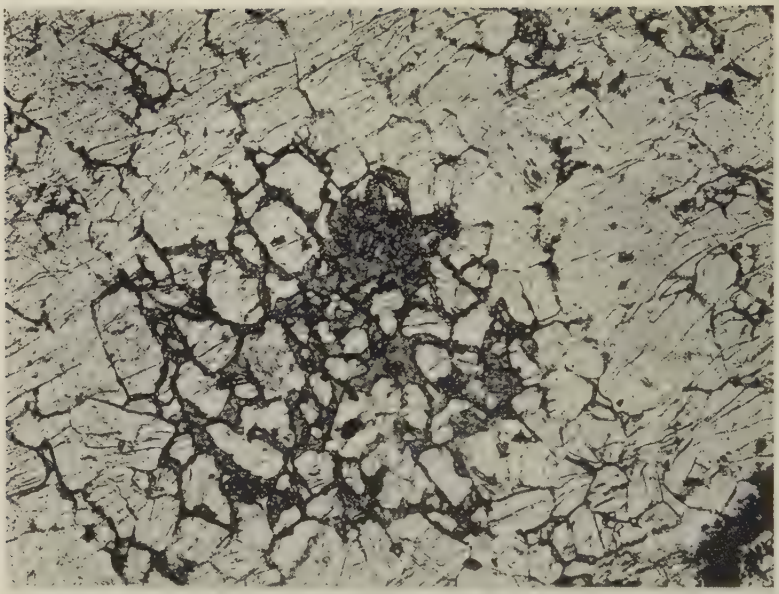

1

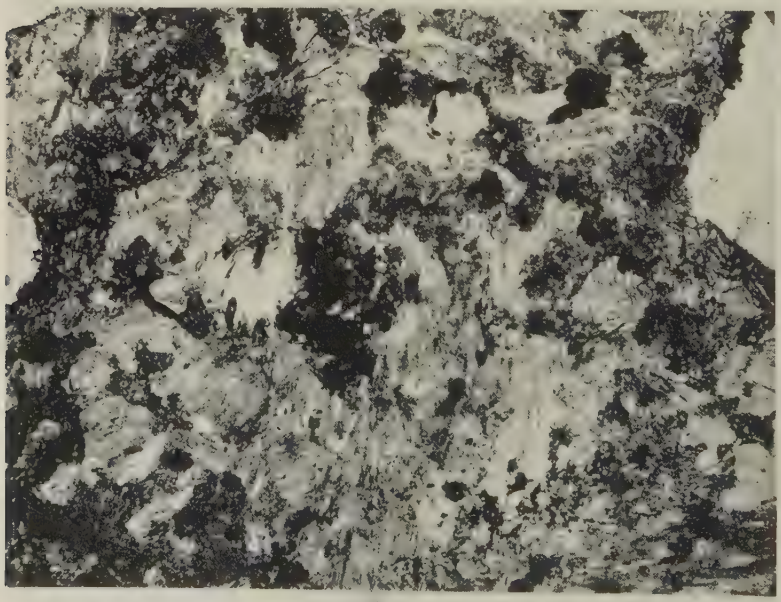

2

S. R. Nockolds: Tilleyite, etc., Ireland.

Subcalcic ferroaugite from Mount Arthur, East Griqualand.

By Arie Poldervaart, M.Sc., Ph.D.
Geology Department, University of Cape Town.

[Communicated by Prof. F. Walker; read March 27, 1947.]

Nomenclature.—In recent years the clinopyroxenes of the system clinoenstatite–diopside–hedenbergite–clinoferrosilite have received a great deal of attention. As research in this field advanced, the need for a balanced and generally acceptable subdivision of the system has made itself increasingly felt. Hess (1941) proposed a classification for these clinopyroxenes, which was subsequently extended by Benson (1944). The present author adopts the main scheme of Benson's classification, but suggests the following minor modifications (fig. 1):

(i) The addition of a new subdivision 'ferrohedenbergite' to counterbalance the endiopside field and to accommodate the end-members of the normal magmatic clinopyroxene series.

(ii) The boundary line between the salite to intermediate pigeonite fields and the ferrosalite to ferropigeonite fields to be drawn as the perpendicular bisector of the En–Fs line.

(iii) The division line between magnesian- and intermediate pigeonite has been moved slightly towards the En–Wo line.

(iv) Benson suggests the lines 2V 45° and 2V 30° as boundaries between (*a*) the augites and ferroaugites, (*b*) their subcalcic equivalents, and (*c*) the pigeonites. The position of these two lines was taken from Tomita's diagram for 2V (1934). In his work on the Karroo dolerites the present author found many discrepancies in the application of Tomita's curves. Hence it is considered likely that the exact position of the lines 2V 45° and 2V 30° will be altered as more data become available.

Benson's suggestion to express compositions of all rock-forming minerals in terms of molecular percentages (1944, p. 76) is welcomed by the author. Thus all compositions of clinopyroxenes in this paper are given as molecular percentages.

Chemical Data.—The analysis of the subcalcic ferroaugite, the calculated atomic ratios to 6(O,OH) atoms, and the estimated formulae are

presented in table I, together with the analysis, norm, and mode of the dolerite-pegmatite from which the pyroxene was obtained. The rock contains tabular plagioclase (An_{46}), euhedral, brown subcalcic ferroaugite, and a dark mesostasis, while titanomagnetite and ovoid patches of chalcedony occur in minor quantities (Poldervaart, 1946).

TABLE I. Chemical analyses. (Analyst, W. H. Herdsman.)

Subcalcic ferroaugite from dolerite-pegmatite of Mount Arthur, East Griqualand.

	Analysis.	100%.		Atomic ratios.			No. mols. on basis 6(O,OH).
SiO_2	49·57	49·67	Si^{IV}	0·828	1·936		1·993
TiO_2	0·78	0·78	Al^{III}	0·028	0·066	0·057	
						0·009	
Al_2O_3	1·36	1·36	Fe^{III}	0·018	0·042		
Fe_2O_3	1·38	1·38	Fe^{II}	0·305	0·714		
FeO	21·92	21·96	Mg^{II}	0·251	0·587		1·992
MnO	0·45	0·45	Ca^{II}	0·257	0·601		
MgO	10·03	10·05	Ti^{IV}	0·010	0·023		
CaO	14·32	14·35	Mn^{II}	0·007	0·016		
Na_2O	trace	100·00	O''	2·565			
K_2O	trace						
H_2O+	0·44	Formula: $(Mg,Fe^{III},Fe^{II},Ca,Ti,Mn,Al)_2[(Si,Al)_2O_6]$					
H_2O-	0·04	$Wo_{31·6}En_{30·9}Fs_{37·5}$					
P_2O_5	trace						
Total	100·29						

Colour, brown; sp. gr. 3·47, α 1·712, γ 1·733, 2V 43°, $\gamma : c = 44°$.

Dolerite-pegmatite of Mount Arthur, East Griqualand.

Analysis.		Norm.			Mode.	
SiO_2	52·52	Qu	13·0		plagioclase	21·5
TiO_2	2·56	Or	7·8		pyroxene	25·9
Al_2O_3	11·26	Ab	14·2		iron-ore	15·5
Fe_2O_3	2·88	An	19·5		mesostasis	36·0
FeO	14·22	Di Wo	6·5		chalcedony	1·1
MnO	0·41	Di En	1·7			100·0
MgO	2·57	Di Fs	5·2			
CaO	7·22	Hy En	4·7			
Na_2O	1·65	Hy Fs	14·9			
K_2O	1·34	Il	5·0			
H_2O+	1·48	Mt	4·2			
H_2O-	1·37	Ap	0·3			
P_2O_5	0·23	H_2O	2·9			
Total	99·71	Total	99·9			

As in most pyroxenes, part of the Al^{III} replaces Si^{IV} in the crystal structure. The analysis is fairly low in sesquioxides and hence the composition may be expressed in terms of Wo, En, and Fs.

Fig. 2 shows clinopyroxenes of similar compositions, plotted against

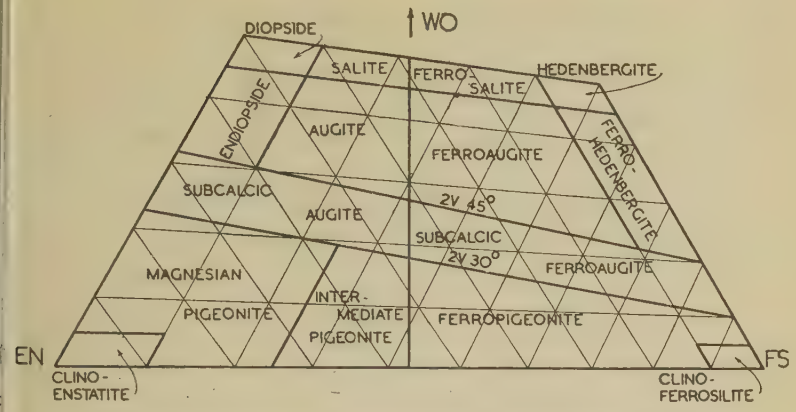

FIG. 1. Nomenclature of the clinopyroxenes of the system En–Di–He–Fs.

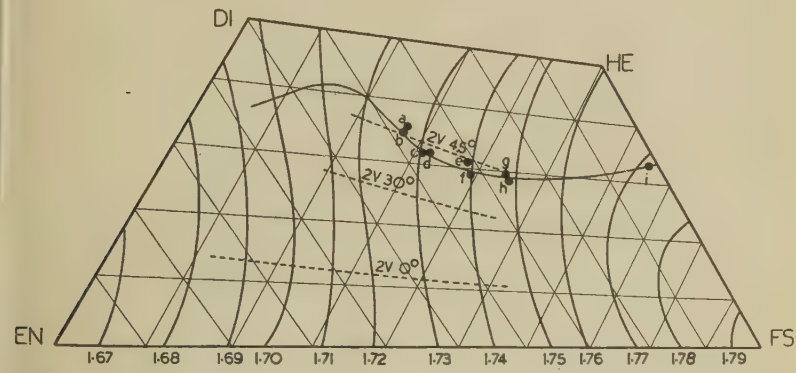

FIG. 2. Plot of refractive index γ and chemical analyses of clinopyroxenes. *a*, Tyne Head (Teall, 1884); *b*, Whin Sill (Teall, 1884); *c*, Skaergaard (Wager and Deer, 1939); *d*, Finland (Wahl, 1906); *e*, Mount Arthur (new analysis); *f*, Volhynia (Lebedev, 1936); *g*, Rocky Hill (Phillips, 1899); *h*, Skaergaard (Wager and Deer, 1939); *i*, Skaergaard (Wager and Deer, 1939).

the γ-curves drawn by Deer and Wager (1938, p. 20, fig. 2) and the course of crystallization of clinopyroxenes according to Hess (1941, p. 585, fig. 10), while the provisional positions of the lines 2V 45°, 30°, and 0° are also indicated.

In table II compositions of the analysed subcalcic ferroaugite are given, as deduced from the optical properties, using the diagrams of Deer and Wager (1938) and Tomita (1934).

TABLE II. Composition of subcalcic ferroaugite.

	Calculated from Chemical analyses.	Deduced from γ index and course of crystallization.	Deduced from γ and α indices.	Deduced from γ and 2V	Deduced from γ and γ:c.	Deduced from 2V and γ:c.
Wo	31·6	30	22	23	19	22
En	30·9	33	39	38	39	28
Fs	37·5	37	39	39	42	50

It appears most accurate to find the composition from the intersection of Deer and Wager's γ-curves with the course of crystallization as given by Hess. The unreliability of the values for 2V and γ:c as a standard for correlation is also clearly demonstrated.

Acknowledgements.—The writer is indebted to Professor F. Walker, of the Cape Town University, Professor W. N. Benson, of the University of Otago, and to Professor H. H. Hess, of Princeton University, for their interest, helpful advice, and stimulating correspondence on the subject of the pyroxenes. The cost of the chemical analysis was met by a grant from the National Research Council, which is here gratefully acknowledged.

Abstract.—A new analysis of a subcalcic ferroaugite is given. The calculated composition is compared with compositions deduced from the optical properties according to various methods. Slight modifications to Benson's nomenclature of the clinopyroxenes are suggested.

BIBLIOGRAPHY.

BENSON (W. N.), 1944. The basic igneous rocks of eastern Otago and their tectonic environment. Trans. Roy. Soc. New Zealand, vol. 74, pp. 71–123. [M.A. **9**-151.]

DEER (W. A.) and WAGER (L. R.), 1938. Two new pyroxenes included in the system clinoenstatite, clinoferrosilite, diopside, and hedenbergite. Min. Mag., vol. 25, pp. 15–22.

HESS (H. H.), 1941. Pyroxenes of common mafic magmas. Amer. Min., vol. 26, pp. 515–535 and 573–594. [M.A. **8**-233.]

LEBEDEV (P. I.), 1936. Beitrag zur Petrographie und Mineralogie der basischen Paegmatite Volyniens. Vernadsky jubilee volume, Acad. Sci. U.S.S.R., vol. 2, pp. 999–1012. [M.A. **7**-198.]

PHILLIPS (A. H.), 1899. Mineralogical structure and chemical composition of the trap of Rocky Hill, New Jersey. Amer. Journ. Sci., ser. 4, vol. 8, pp. 267–285.

POLDERVAART (A.), 1946. The petrology of the Mount Arthur dolerite complex, East Griqualand. Trans. Roy. Soc. South Africa, vol. 31, pp. 83–110.

SHANNON (E. V.), 1924. The mineralogy and petrology of intrusive Triassic diabase at Goose Creek, Loudoun County, Virginia. Proc. U.S. National Museum, vol. 66, art. 2, pp. 1–86. [M.A. **3**-204.]

Teall (J. J. H.), 1884. On the chemical and microscopical characters of the Whin Sill. Quart. Journ. Geol. Soc. London, vol. 40, pp. 640–657.

Tomita (T.), 1934. Variations in optical properties, according to chemical composition, in the pyroxenes of the clinoenstatite–clinohypersthene–diopside-hedenbergite system. Journ. Shanghai Sci. Inst., Sect. 3, vol. 1, pp. 41–58. [M.A. **6**–71.]

Wager (L. R.) and Deer (W. A.), 1939. Geological Investigations in east Greenland. Part III. The petrology of the Skaergaard intrusion, Kangerdlugssuaq, east Greenland. Meddelelser om Grønland, vol. 105, no. 4, 352 pp. [M.A. **8**–27.]

Wahl (W.), 1906. Ueber einen Magnesiumdiopsidführenden Diabas von Källsholm, Skärgård von Föglö, Ålandsinseln. Festschrift H. Rosenbusch, Stuttgart, pp. 399–412.

The relationship of orthopyroxene to pigeonite.

(With Plate XIII.)

By Arie Poldervaart, M.Sc., Ph.D.
Geology Department, University of Cape Town.

[Communicated by Prof. F. Walker; read March 27, 1947.]

Introduction.—Interest in the orthopyroxene series is evidenced by the great number of publications on that subject which appeared in the literature. Correlations of the chemical composition and optical properties were attempted by Winchell (1923, 1933), Walls (1935), Henry (1935), and Hess and Phillips (1940). The nomenclature of the series was discussed by Winchell (1923), Alling (1936), and Hess and Phillips (1940). The obscure phenomena exhibited by certain orthopyroxenes in polarized light, attributed by some to twinning, by others to exsolution, was noted by a great many petrologists, of whom are mentioned here Lewis (1908), Holmes and Harwood (1928), Guimarães (1933), Scholtz (1936), Hess and Phillips (1938, 1940), Kuschke (1939), Wager and Deer (1939), Nel (1940), Walker (1940, 1943), Walker and Poldervaart (1940, 1941), Edwards (1942), Henry (1942), and Poldervaart (1944, 1946). Other authors are mentioned by Henry (1942). Attempts to define the stability fields of orthopyroxenes and pigeonites were made by Hess (1941), Walker (1940, 1943), Walker and Poldervaart (1941), Edwards (1942), and Poldervaart (1944, 1946).

The present research partly confirms and extends previously expressed views, and is partly an attempt to summarize the present-day knowledge of this group of rock-forming minerals.

Nomenclature.—It appears most logical to subdivide the three series of solid solutions, formed by the most common groups of rock-forming minerals (i.e., the plagioclase, olivine, and orthopyroxene series) in an analogous manner. The subdivision of the plagioclase series is now generally accepted. Deer and Wager (1939) proposed a similar classification for the olivine series. It is here suggested to subdivide the orthopyroxene series in like manner (text-fig. 1).

The proposed subdivision of the series necessitates a new name to cover the range Of_{70-90}. Since analysed orthopyroxenes within this

range have been described mainly from eulysites, the name 'eulite' is here proposed.

Chemical data.—Two new analyses of magnesian orthopyroxenes, their atomic ratios to 6(O,OH) atoms, and the estimated formulae[1] are given in table I.

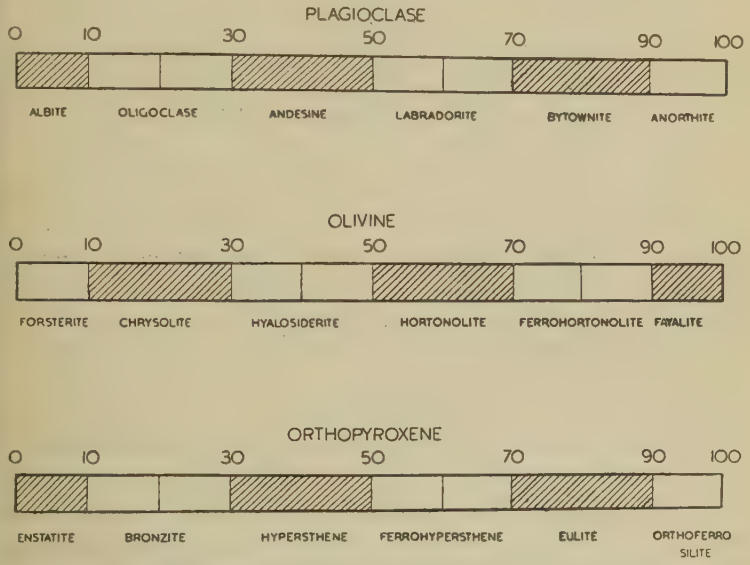

Text-fig. 1. Nomenclature of the plagioclase, olivine, and orthopyroxene series. (Molecular percentages.)

The object of the analyses was to test the statements of Hess and Phillips (1938, 1940) regarding the lime content of orthopyroxenes. Hence extreme care was taken to ensure purity in the samples submitted for analysis. In both cases the material was hand-picked and checked repeatedly under the microscope.

The Hanover bronzite forms large 'phenocrysts' (average length 1·5—2·5 mm.) in a medium-grained, ophitic olivine-dolerite (Walker and Poldervaart, 1942). Most of the crystals show a peculiar patchy extinction in polarized light, but some exhibit the 'graphic intergrowth' on an extremely fine scale along their margins (pl. XIII, fig. 1). The Rustenburg norite was obtained from the Schilpadnest mine, Rustenburg, and occurred in the upper part of the Merensky Reef, immediately

[1] Conforming to earlier practice (Henry, 1935; Hess and Phillips, 1940) molecular proportions of MnO were added to those of FeO in calculating the compositions. All other admixtures were neglected.

TABLE I. Chemical analyses of bronzite. (Analyst, W. H. Herdsman.)

Bronzite from Karroo dolerite at Hanover, Cape Province.

	Analysis.	100%.		Atomic ratios.			No. mols. on basis 6(O,OH).
SiO_2	... 52·86	53·33	$Si^{\cdot\cdot\cdot\cdot}$	...	0·889	1·898	1·996
TiO_2	... 0·26	0·26	$Al^{\cdot\cdot\cdot}$	...	0·081	0·173 (0·098, 0·075)	
Al_2O_3	... 4·08	4·12	$Fe^{\cdot\cdot\cdot}$	...	0·016	0·034	1·995
Fe_2O_3	... 1·26	1·27	$Fe^{\cdot\cdot}$	...	0·157	0·336	
FeO	... 11·23	11·33	$Mg^{\cdot\cdot}$	...	0·677	1·444	
MnO	... 0·23	0·23	$Ca^{\cdot\cdot}$	...	0·043	0·092	
MgO	... 26·82	27·06	$Mn^{\cdot\cdot}$	...	0·003	0·007	
CaO	... 2·38	2·40	$Ti^{\cdot\cdot\cdot\cdot}$	...	0·003	0·007	
Na_2O	... trace	—	$O^{\prime\prime}$	...	2·810		
K_2O	... trace	—	Formula: $(Mg,Fe^{\cdot\cdot\cdot},Ca,Mn,Ti,Al)[(Si,Al)_2O_6]$				
P_2O_5	... nil	—	$Wo_{4\cdot7}En_{76\cdot9}Fs_{18\cdot2}$ or $Of_{19\cdot1}$				
H_2O+	... 0·53	100·00					
H_2O-	... 0·07						
Total	... 99·72						

Colour, green; pleochroism none; sp. gr. 3·42, α 1·680, γ 1·692, $2V_\alpha$ 77°.

Bronzite from Bushveld norite at Rustenburg, Transvaal.

	Analysis.	100%.		Atomic ratios.			No. mols. on basis 6(O,OH).
SiO_2	... 54·26	54·62	$Si^{\cdot\cdot\cdot\cdot}$	...	0·910	1·936	1·998
TiO_2	... trace	—	$Al^{\cdot\cdot\cdot}$	...	0·030	0·064 (0·062, 0·002)	
Al_2O_3	... 1·53	1·54	$Fe^{\cdot\cdot\cdot}$	...	0·020	0·043	1·998
Fe_2O_3	... 1·56	1·57	$Fe^{\cdot\cdot}$	...	0·164	0·349	
FeO	... 11·71	11·79	$Mg^{\cdot\cdot}$	...	0·744	1·583	
MnO	... 0·43	0·43	$Ca^{\cdot\cdot}$	...	0·004	0·008	
MgO	... 29·68	29·87	$Mn^{\cdot\cdot}$	...	0·006	0·013	
CaO	... 0·18	0·18	$Ti^{\cdot\cdot\cdot\cdot}$	...	—	—	
Na_2O	... nil	—	$O^{\prime\prime}$	...	2·813		
K_2O	... nil	—	Formula: $(Mg,Fe^{\cdot\cdot\cdot},Fe^{\cdot\cdot},Ca,Mn,Al)[(Si,Al)_2O_6]$				
P_2O_5	... nil	—	$Wo_{0\cdot4}En_{81\cdot1}Fs_{18\cdot3}$ or $Of_{18\cdot6}$				
H_2O+	... 0·42	100·00					
H_2O-	... 0·09						
Total	... 99·86						

Colour, brown; pleochroism moderate; sp.gr. 3·40, α 1·679, γ 1·691, $2V_\alpha$ 77°.

below the upper chrome band. A few of the crystals show sporadic exsolution lamellae, but the majority exhibit extremely fine lamellar twinning (pl. XIII, fig. 2) of the type described by Henry (1942) and Scholtz (1936).

Correlation of optical properties and chemical composition.—Text-fig. 2 shows the variation in optical properties with chemical composition. The data used are given in table II.

Orthopyroxene–pigeonite stability fields.—Various authors have commented on the abnormal behaviour in polarized light of orthopyroxenes within the range Of_{15-35}. In basalts the mineral generally extinguishes quite normally. In dolerites the orthopyroxene may show a peculiar uneven extinction, or more commonly, sets of finely ruled lamellae and irregular blebs of a mineral of different extinction and double refraction than the orthopyroxene host (pl. XIII, figs. 1 and 3). The structure may occur over the entire crystal, or only in its centre, or confined to the margins. Following Walker (1940), the phenomenon is called the

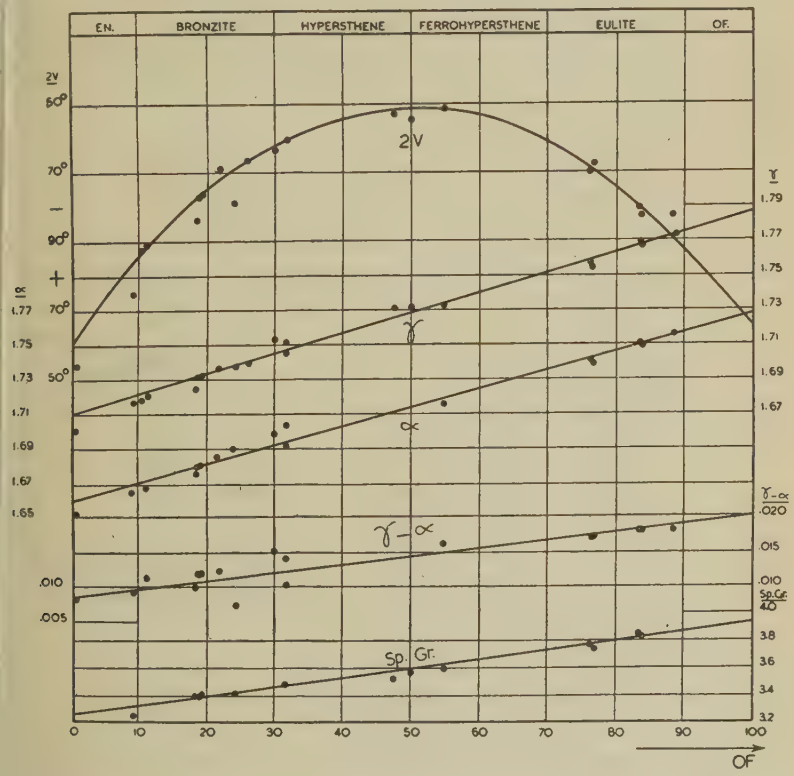

TEXT-FIG. 2. Optical properties and chemical composition of the orthopyroxene series. (Molecular percentages.)

'graphic intergrowth', and the patchy extinction, sometimes observed, is regarded as representing the 'graphic intergrowth' on a submicroscopic scale.

TABLE II. Chemical analyses of orthopyroxenes calculated to 100% and arranged in order of mol.% of orthoferrosilite (Of).

Ref. Number	1.	2.	3.	4.	5.	6.	7.	8.	9.	10.
SiO_2 ...	59·8	57·1	53·8	55·9	53·7	54·6	53·3	52·0	51·6	53·6
TiO_2 ...	—	—	0·1	—	0·1	—	0·3	—	0·8	0·3
Al_2O_3 ...	—	0·9	1·7	1·7	4·5	1·5	4·1	3·9	2·2	2·2
Fe_2O_3 ...	—	0·4	1·5	1·4	0·3	1·6	1·3	—	4·5	0·8
FeO ...	0·4	6·4	6·7	7·2	11·6	11·8	11·3	13·3	13·9	15·3
MnO ...	—	—	0·2	0·2	0·2	0·4	0·2	0·6	0·2	0·3
MgO ...	39·5	34·9	33·2	32·5	29·2	29·9	27·1	27·5	24·5	24·7
CaO ...	0·3	0·1	2·3	0·7	0·4	0·2	2·4	2·0	1·9	2·6
Na_2O ...	—	0·2	—	—	—	—	—	—	0·4	0·1
K_2O ...	—	—	0·1	—	—	—	—	—	—	—
P_2O_5 ...	—	—	—	0·1	—	—	—	—	—	—
Cr_2O_3 ...	—	—	0·4	0·3	—	—	—	0·7	—	0·1
2V ...	54° (+)	75° (+)	87° (+)	89° (+)	84° (−)	77° (−)	77° (−)	69° (−)	n.d.	66° (−)
α ...	1·651	1·666	n. d.	1·668	1·675	1·679	1·680	1·681	1·690	n. d.
γ ...	1·659	1·675	1·677	1·679	1·685	1·691	1·692	1·696	1·700	1·699
γ−α ...	0·008	0·009	—	0·011	0·010	0·012	0·012	0·015	0·010	—
Sp. gr.	n. d.	3·25	n.d.	n. d.	3·40	3·40	3·42	n. d.	3·42	n. d.
Of. (mol. %)	0·6	9·3	10·4	11·2	18·3	18·6	19·1	21·9	24·2	26·0

11.	12.	13.	14.	15.	16.	17.	18.	19.	20.	21.
51·5	52·0	53·2	50·0	50·0	50·6	48·2	47·9	47·4	46·4	46·5
0·9	0·4	0·2	0·6	0·4	0·3	—	0·1	—	0·2	0·1
0·5	1·7	1·4	3·6	2·8	1·9	0·7	1·5	0·1	0·3	0·9
0·8	3·2	1·1	—	1·9	2·1	1·3	0·5	0·3	0·2	0·3
19·5	18·3	18·7	26·7	27·5	29·7	37·8	35·7	42·1	45·0	42·1
0·1	0·4	0·9	0·5	0·6	0·2	2·5	6·3	3·9	1·2	5·1
25·1	22·2	23·3	16·8	15·6	13·8	7·0	7·1	5·1	5·1	3·5
1·0	1·8	1·2	1·2	0·9	1·4	2·5	0·9	1·1	1·6	1·5
0·4	—	—	0·1	0·1	—	—	—	—	—	—
0·2	—	—	0·2	0·2	—	—	—	—	—	—
—	—	—	0·3	—	—	—	—	—	—	—
—	—	—	—	—	—	—	—	—	—	—
63° (−)	n. d.	60° (−)	53°	55°	51° (−)	70° (−)	68° (−)	81° (−)	83° (−)	83° (+)
1·698	1·702	1·691	n. d.	n. d.	1·715	1·740	1·738	1·750	1·751	1·755
1·713	1·712	1·705	1·730	1·731	1·731	1·757	1·755	1·768	1·769	1·773
0·015	0·010	0·014	—	—	0·016	0·017	0·017	0·018	0·018	0·018
n. d.	3·48	n. d.	3·53	3·56	3·60	3·77	3·75	3·83	3·84	3·88
30·2	31·9	31·9	47·4	50·0	54·7	76·2	76·6	83·3	83·4	88·2

1, Enstatite, Shallowater meteorite (Hess and Phillips, 1940). 2, Enstatite, Espedalen, Norway (Washington and Merwin, 1923). 3, Enstatite, Stillwater, Montana (Hess and Phillips, 1940). 4, Enstatite, Webster, North Carolina (Hess and Phillips, 1940). 5, Lapland (Mikkola and Sahama, 1937). 6, Bronzite, Rustenburg, Transvaal (this paper). 7, Bronzite, Hanover, Cape (this paper). 8, Johnstown meteorite (Hovey, 1925). 9, Hypersthene, Nain, Labrador (Washington and Merwin, 1923). 10, Hypersthene, Stillwater, Montana (Hess and Phillips, 1940). 11, Hypersthene, Komagataké, Japan (Közu, 1934). 12, Hypersthene, Summitville, Colorado (Larsen, Irving, and Gonyer, 1936). 13, Hypersthene, Odawara-mati, Japan (Kuno, 1938). 14, and 15, Hypersthene, Quilquox, Aberdeenshire (Walls, 1935). 16, Hypersthene, Glen Buchat, Aberdeenshire (Henry, 1935). 17, Iron-hypersthene, Vittinki, Finland (Saxén, 1925; Henry, 1935). 18, Hypersthene, Loch Duich, Ross-shire (Henry, 1935). 19, Hypersthene, Tunaberg, Sweden (Sundius, 1932). 20, Mansjö, Sweden (Henry, 1935). 21, Hypersthene, Manchuria (Tsuru and Henry, 1937).

In norites the orthopyroxene frequently shows one, two, or three sets of well-developed lamellae, while the irregular blebs are absent. The

structure is on a much coarser scale and more regular than the 'graphic intergrowth'. Following Hess and Phillips (1938), it is termed the 'lamellar intergrowth' (pl. XIII, fig. 4).

A great deal of confusion has been caused by the occurrence of fine lamellar twinning in orthopyroxenes (pl. XIII, fig. 2), which is often very similar in appearance to the 'graphic intergrowth'. Twinning of this type was described by Scholtz (1936) and Henry (1942), while it is also exhibited by the Rustenburg bronzite. Henry ascribes the structure to deformation during crystallization.

The patchy extinction, 'graphic intergrowth', or 'lamellar intergrowth' is caused by exsolution of lime. The present author agrees with Hess and Phillips (1938, 1940) that the structure is produced in either of two ways, viz.:

(*a*) By the inversion of earlier-formed, unstable pigeonite to orthopyroxene upon slow cooling, accompanied by the expulsion of lime from the molecule.

(*b*) By the exsolution of $CaSiO_3$, dissolved in the orthopyroxene molecule, likewise on further slow cooling.

The relative stabilities of orthopyroxene and pigeonite are rather closely linked under magmatic conditions. Pigeonite appears to be the stable phase at high temperatures, but is unstable at lower temperatures, when orthopyroxene becomes the stable phase (Hess, 1941). Thus, on quick cooling, pigeonite is preserved in a metastable condition, while slow cooling results in the inversion of pigeonite to orthopyroxene with the 'graphic' or 'lamellar' intergrowth.

Pigeonite remains the stable phase at all temperatures in the presence of high volatile concentrations, orthopyroxene becoming unstable under such conditions. This relationship is demonstrated by the following facts:

(i) Dolerite-pegmatites may contain pigeonite, but there is no record of dolerite-pegmatites in which orthopyroxene occurs.

(ii) Granophyres, formed in the Karroo by the metasomatism of siltstones by dolerite magma (Walker and Poldervaart, 1942), may contain pigeonite, but orthopyroxene is absent.

(iii) At Mount Arthur, tholeiites evolved from olivine-dolerites through the distillation of water from large sedimentary xenoliths, contain pigeonite, but no orthopyroxene (Poldervaart, 1946).

If magmatic conditions move towards the stability field of pigeonite, by a gradual concentration of volatile elements, orthopyroxene

crystallizes with an increasing amount of dissolved lime, which is again exsolved on cooling. Such conditions prevailed in the Palisade sill (Walker, 1940), the Whin sill (Holmes and Harwood, 1928), the Hangnest sill (Walker and Poldervaart, 1941) and the Sedgewick laccolith (Edwards, 1942). These intrusions all carry pigeonite in their upper portions, while orthopyroxene occurs in the lower parts. The last three intrusions are typical bronzite-dolerites with chilled phases containing phenocrysts of bronzite. From the lower contact upwards the 'graphic intergrowth' first appears along the margins of the orthopyroxene crystals, then covers their entire surface, and finally pigeonite occurs instead of orthopyroxene.

The relations of magnesian orthopyroxene and pigeonite (Mg:Fe ratio 4:1) are further summarized in table III.

TABLE III. Conditions of formation of magnesian orthopyroxene and pigeonite.

Temperature of magma (Hess, 1941).	First mineral to crystallize.	Condition of magma.	Rate of cooling.	
<1100° Slow rate of crystallization	Normal bronzite	dry	slow, fast	Normal bronzite
		wet	slow	Bronzite with graphic intergrowth → Pigeonite
			fast	'Frozen' as normal bronzite or bronzite with graphic intergrowth
±1100° High rate of crystallization	Bronzite with dissolved lime up to 9% $CaSiO_3$	dry	slow	Bronzite with graphic intergrowth → Normal bronzite
			fast	'Frozen' as lime-bronzite (*unstable*) or as bronzite with graphic intergrowth
		wet	slow	Bronzite with graphic intergrowth → Pigeonite
			fast	'Frozen' as lime-bronzite (*unstable*) or as bronzite with graphic intergrowth
>1100°	Pigeonite	dry	slow	Bronzite with graphic intergrowth → Normal bronzite
			fast	'Frozen' as pigeonite (*unstable*) or as bronzite with graphic intergrowth
		wet	slow, fast	Pigeonite

Acknowledgements.—The writer is indebted to Professor F. Walker of the Cape Town University, for his interest and advice in the present research. The cost of the chemical analyses was met by a grant from the National Research Council, which is here gratefully acknowledged.

Abstract.—A new classification of the orthopyroxene series is suggested. Two analyses of magnesian orthopyroxenes are given, and curves are drawn to correlate the chemical composition with the optical properties. The stability fields of orthopyroxenes and pigeonites are discussed in detail.

Bibliography.

Alling (H. L.), 1936. Interpretative petrology of the igneous rocks. New York.

Deer (W. A.) and Wager (L. R.), 1939. Olivines from the Skaergaard intrusion, Kangerdlugssuak, east Greenland. Amer. Min., vol. 24, pp. 18–25. [M.A. **7**–447.]

Edwards (A. B.), 1942. Differentiation of the dolerites of Tasmania. Journ. Geol. Chicago, vol. 50, pp. 451–480 and 579–610. [M.A. **9**–161.]

Guimarães (D.), 1933. A província magmática do Brasil meridional. Serviço Geológico, Minas Geraes, Monogr. 1, pp. 43–64.

Henry (N. F. M.), 1935. Some data on the iron-rich hypersthenes. Min. Mag., vol. 24, pp. 221–226.

—— 1942. Lamellar structure in orthopyroxenes. Min. Mag., vol. 26, pp. 179–188.

Hess (H. H.), 1941. Pyroxenes of common mafic magmas. Amer. Min., vol. 26, pp. 515–535 and 573–594. [M.A. **8**–233.]

—— and Phillips (A. H.), 1938. Orthopyroxenes of the Bushveld type. Amer. Min., vol. 23, pp. 450–456. [M.A. **7**–180.]

—— —— 1940. Optical properties and chemical composition of magnesian orthopyroxenes. Amer. Min., vol. 25, pp. 271–285. [M.A. **8**–18.]

Holmes (A.) and Harwood (H. F.), 1928. The age and composition of the Whin sill and the related dikes of the north of England. Min. Mag., vol. 21, pp. 493–542.

Hovey (E. O.), 1925. A new meteoric stone from Johnstown, Weld County, Colorado. Amer. Mus. Novitates, no. 203. [M.A. **3**–256.]

Kôzu (S.), 1934. The great activity of Komagataké in 1929. Min. Petr. Mitt. (Tschermak), vol. 45, pp. 133–174. [M.A. **6**–21.]

Kuno (H.), 1938. Hypersthene from Odawara-mati, Japan. Proc. Imp. Acad. Tokyo, vol. 14, pp. 218–220. [M.A. **7**–180.]

Kuschke (G. S. J.), 1939. The critical zone of the Bushveld igneous complex, Lydenburg district. Trans. Geol. Soc. South Africa, 1940, vol. 42 (for 1939), pp. 57–81. [M.A. **8**–33.]

Larsen (E. S.), Irving (J.), Gonyer (F. A.), and Larsen (E. S., 3rd.), 1936. Petrologic results of a study of the minerals from the Tertiary volcanic rocks of the San Juan region, Colorado. Amer. Min., vol. 21, pp. 679–701. [M.A. **7**–31.]

Lewis (J. V.), 1908. The petrography of the Newark igneous rocks of New Jersey. Ann. Rep. State Geol. N.J., for 1906, pp. 97–167.

Mikkola (E.) and Sahama (T. G.), 1937. The region to the south-west of the "granulite series" in Lapland and its ultrabasics. Bull. Comm. Géol. Finlande, no. 115, pp. 357–371.

Nel (H. J.), 1940. The basal rocks of the Bushveld igneous complex, north of Pretoria. Trans. Geol. Soc. South Africa, 1941, vol. 43 (for 1940), pp. 37–68. [M.A. **9**–178.]

Poldervaart (A.), 1944. The petrology of the Elephant's Head dike and the New Amalfi sheet (Matatiele). Trans. Roy. Soc. South Africa, vol. 30, pp. 85–119.

—— 1946. The petrology of the Mount Arthur complex (East Griqualand). Trans. Roy. Soc. South Africa, vol. 31, pp. 83–110.

Saxén (M.), 1925. Om mangan-järnmalmfyndigheten i Vittinki. Fennia, Bull.-Soc. Géogr. Finlande, vol. 45, no. 11, p. 18.

Scholtz (D. L.), 1936. The magmatic nickeliferous ores of East Griqualand and Pondoland. Trans. Geol. Soc. South Africa, 1937, vol. 39 (for 1936), pp. 81–210. [M.A. **6**–440.]

Sundius (N.), 1932. Über den sogenannten Eisenanthophyllit der Eulysite. Årsbok Sveriges Geol. Undersökning, vol. 26, no. 2, pp. 1–8. [M.A. **6**–118.]

Tsuru (K.) and Henry (N. F. M.), 1937. An iron-rich, optically-positive hypersthene from Manchuria. Min. Mag., vol. 24, pp. 527–528.

Wager (L. R.) and Deer (W. A.), 1939. Geological investigations in east Greenland, Part III. The petrology of the Skaergaard intrusion, Kangerdlugssuaq, east Greenland. Meddelelser om Grønland, vol. 105, no. 4, 352 pp. [M.A. **8**–27.]

Walker (F.), 1940. The differentiation of the Palisade diabase, New Jersey. Bull. Geol. Soc. Amer., vol. 51, pp. 1059–1106.

—— 1943. Note on the pyroxenes of basaltic magma. Amer. Journ. Sci., vol. 241, pp. 517–520. [M.A. **9**–151.]

—— and Poldervaart (A.), 1940. The petrology of the dolerite sill of Downes Mountain, Calvinia. Trans. Geol. Soc. South Africa, 1941, vol. 43 (for 1940), pp. 159–173.

—— —— 1941. The Hangnest dolerite sill, S. Africa. Geol. Mag., vol. 78, pp. 429–450.

—— —— 1942. The metasomatism of Karroo sediments by dolerite. Trans. Roy. Soc. South Africa, vol. 29, pp. 285–307.

—— —— 1942. The petrology of the Karroo dolerites between Sutherland and Middelburg, C.P. Trans. Geol. Soc. South Africa, 1943, vol. 45 (for 1942), pp. 55–64. [M.A. **9**–179.]

Walls (R.), 1935. A critical review of the data for a revision of the enstatite-hypersthene series. Min. Mag., vol. 24, pp. 165–172.

Washington (H. S.), and Merwin (H. E.), 1923. Note on enstatite, hypersthene, and actinolite. Amer. Min., vol. 8, pp. 63–67. [M.A. **2**–305.]

Winchell (A. N.), 1923. Studies in the pyroxene group. Amer. Journ. Sci., ser. 5, vol. 6, pp. 504–520. [M.A. **2**–219.]

—— 1933. Elements of optical mineralogy, part II. 3rd edit., New York. [M.A. **5**–337.]

Explanation of Plate XIII.

(All crossed nicols.)

Fig. 1. Patchy extinction of bronzite 'phenocryst' in dolerite from Hanover, Cape Province. ×15.

Fig. 2. Lamellar twinning of bronzite in norite from Rustenburg, Transvaal. ×38.

Fig. 3. Graphic intergrowth of bronzite in diabase from Palisade, New Jersey. ×38.

Fig. 4. Lamellar intergrowth of bronzite in norite from Bushveld, Transvaal. ×38.

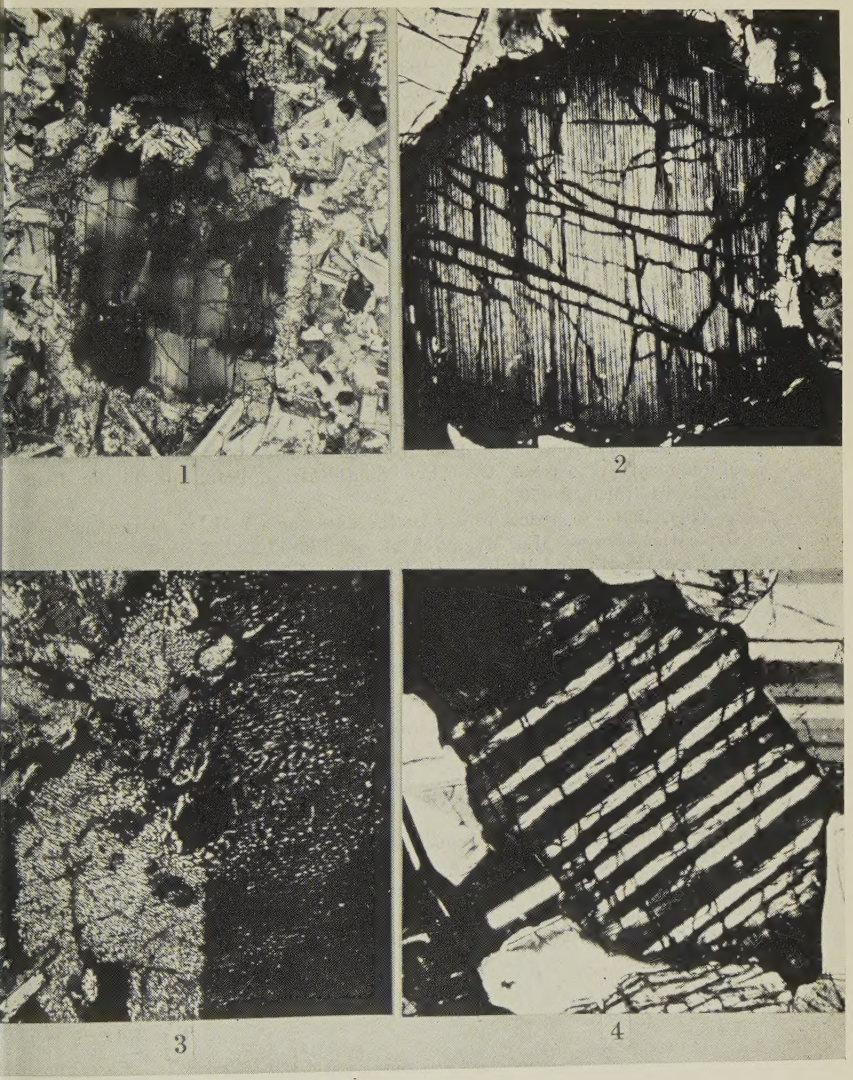

1 2

3 4

A. Poldervaart: Orthopyroxenes.

Chemical analysis of ullmannite from New Brancepeth, Co. Durham

By J. A. Smythe, Ph.D., D.Sc.

[Read June 26, 1947.]

THE first occurrence of this mineral in Britain was announced by L. J. Spencer[1] who found it in the great baryte-witherite vein at New Brancepeth, near Durham. It was found later by Sir Arthur Russell[2] in the witherite vein at Settlingstones, Northumberland.

Spencer proved the presence of antimony in considerable quantity and of sulphur, and returned the nickel as 27·87 %, a quantity which agrees well with the accepted formula, NiSbS; the specific gravity was given as 6·70. In view of the rarity of the mineral and its scientific interest, a complete analysis was deemed advisable, and I have carried this out on a specimen from New Brancepeth, which came into my hands not long after its discovery.

This specimen contained some calcite, which was removed as far as possible by hand-picking the coarsely crushed material; though this was not entirely successful as the analysis showed the presence of 1·57 % of calcium carbonate. There was also 3·93 % of lead present as galena and, rather surprisingly, cold water extracted from the finely powdered mineral no less than 0·9 % of ferrous sulphate. Solution of the mineral in aqua regia left a small residue of quartz. The complete analysis given below shows 8·71 % of these four adventitious constituents; the mode of combination of the remaining 90·93 % will be discussed shortly.

Ni	... ...	23·44	
Fe	... ...	2·94	
Sb	... ...	49·74	
As	... ...	0·95	
S	... ...	13·86	
$FeSO_4.7H_2O$	...	0·90	
$CaCO_3$	...	1·57	
PbS	... ...	4·54	
SiO_2	... ...	1·70	
		99·64	
Sp. gr.	...	6·73	

A section of the polished mineral, examined microscopically in reflected light, did not show the parallel intergrowth of galena and ull-

[1] L. J. Spencer, Min. Mag., 1910, vol. 15, p. 302.
[2] A. Russell, Min. Mag., 1927, vol. 21, p. 383.

mannite observed by Spencer. The galena and calcite occurred together as an infilling of cracks in the ullmannite, and in places the galena could be seen as idiomorphic crystals in the matrix of calcite. There was no evidence of pyritic minerals, so that it may be inferred that the iron and arsenic with their equivalent of sulphur were not present as pyrite, pyrrotine, or mispickel. The origin of the ferrous sulphate is thus, probably, from an external source; in other words, it is an infiltrated addition. Arsenic is clearly in isomorphous association with antimony, and a similar relationship may be accepted for iron and nickel. These inferences are confirmed by the simple relationship between the following molecular ratios:

$$(Ni,Fe):(Sb,As):S = 1{\cdot}05:1:1{\cdot}01$$

and the formula of the mineral may thus be expressed as (Ni,Fe)(Sb,As)S. Deducting impurities and calculating to 100%, the composition of the mineral is given under I, and the calculated composition for the simple formula NiSbS under II.

	I.	II.
Ni	25·8	27·6
Fe	3·2	—
Sb	54·7	57·3
As	1·0	—
S	15·3	15·1
	100·0	100·0